

Article

The Effects of Chloride on the High-Temperature Pressure Oxidation of Chalcopyrite: Some Insights from Batch Tests—Part 1: Leach Chemistry

Robbie G. McDonald 

CSIRO Mineral Resources, Australian Minerals Research Centre, 7 Conlon Street, Waterford, WA 6152, Australia; robbie.mcdonald@csiro.au

Abstract: The complete reaction of chalcopyrite at ≥ 220 °C under pressure oxidation conditions (10 or 20% *w/w* pulp density, PO₂ 700 kPa) is a clean, near complete process, yielding high copper extractions (~99%) in an acidic leach liquor composed of dissolved metal sulphates, when high-quality process water is employed. However, when the process water contains chloride ions, here 3–100 g/L, although the copper extraction rate is enhanced, complete oxidation of sulphur under batch processing conditions is delayed. Chloride addition, therefore, appears to favour an oxidation mechanism that liberates cupric ions and preferentially forms elemental sulphur over sulphate. This provides evidence for the decoupling of the copper extraction and sulphate formation reactions. Increasing the reaction temperature, here to 245 °C, increases the rate of sulphuric acid formation and decreases the iron concentration in the leach liquor. The study also examines the effects of various upfront acid and other salt additions upon copper extraction. Added sulphuric acid was shown to slow the reaction, whereas salts such as cupric chloride and sodium sulphate had small effects on the rate and extent of copper extraction.

Keywords: chalcopyrite; chloride; pressure oxidation



Citation: McDonald, R.G. The Effects of Chloride on the High-Temperature Pressure Oxidation of Chalcopyrite: Some Insights from Batch Tests—Part 1: Leach Chemistry. *Minerals* **2023**, *13*, 1065. <https://doi.org/10.3390/min13081065>

Academic Editor: Jean-François Blais

Received: 27 June 2023

Revised: 4 August 2023

Accepted: 8 August 2023

Published: 11 August 2023



Copyright: © 2023 by the author. Licensee MDPI, Basel, Switzerland. This article is an open access article distributed under the terms and conditions of the Creative Commons Attribution (CC BY) license (<https://creativecommons.org/licenses/by/4.0/>).

1. Introduction

Hydrometallurgical copper extraction from chalcopyrite at relatively low temperatures can be problematic, although historically, several processes, including Duval's CLEAR Process [1], the Cuprex process [2], the Intec Process [3], the Albion Process [4], Outokumpu's HydroCopper Process (e.g., [5]), and the Galvanox process (e.g., [6]), have been developed beyond the bench scale. More recently, the FLSmidth® Rapid Oxidative Leach (ROL) process [7–9], and an alkaline glycine-based process developed at Curtin University [10], have been applied to chalcopyrite-containing materials. Successful application was also demonstrated for the Activox® Process [11]; however, the closure of the Tahti Demonstration Plant appears to have signalled a halt to further development of this technology for the processing of base metal sulphides.

Many reviews that examine chalcopyrite processing have appeared. Subramanian and Jennings [12] appear to have been the first to review hydrometallurgical processing of chalcopyrite concentrates. Dutrizac [13] reviewed earlier chloride-assisted processes in some detail, Venkatachalam [14] and Prasad and Pandey [15] examined hydrometallurgical routes both with and without pre-treatment, Berezowsky and Trytten [16] considered the commercialization of leaching processes, while Dreisinger [17,18] and Baba [19] provided more recent, general overviews of copper leaching from sulphides, and in particular chalcopyrite. Klauber [20] focused on chalcopyrite surface chemistry during leaching in acidic sulphate environments, Córdoba et al. [21,22] focused on the leaching of chalcopyrite by ferric iron, while the fundamentals of chalcopyrite leaching have also been reviewed by Li et al. [23]. Atmospheric leaching of chalcopyrite using identified lixiviant systems has been reviewed by Watling [24,25]. The application of novel lixiviants, including ionic

liquids, glycine, and methane sulfonic acid, and those historically considered but largely examined only in laboratory studies (including ammonia and hypochlorite systems), was recently reviewed by Barton and Hiskey [26].

Almost twenty years ago, Freeport McMoRan commenced a program to investigate higher-temperature technologies for processing copper concentrates, including chalcopyrite. The world's first commercial application of high-temperature pressure leaching and operating at 225 °C was demonstrated at the Bagdad operation several years later [27], with the acid produced employed to irrigate test heaps. Subsequently, a demonstration plant operating a medium-temperature (160 °C), partial oxidation process, employing fine grinding and surfactant, was run at the Morenci site [28]. After shutting down in 2008, this circuit was restarted in high-temperature mode (200 °C) in 2015 and has been operating since, also generating acid for low-grade ore leaching [29]. Recently, the commercial application of the Albion Process to refractory copper concentrates unsuitable or uneconomic for smelting, and which dates to 2014, was described for the Sable processing plant in Zambia [30].

Other pressure oxidation technologies, including the CESL (e.g., [31]) and Platsol[®] (e.g., [32,33]) processes, continue to be developed. While the focus of these processes is not specifically on chalcopyrite leaching, there are some interesting parallels with the present study, considering their use of chloride.

The FLSmidth[®] ROL process employs copper activation in a stirred media reactor to mitigate surface passivation issues and enable >95% copper extraction from chalcopyrite within 6 h [7,8]. Karcz et al. [34] reports the relationship between copper activation/pre-conditioning and the conversion of the surface layers and deformation of the chalcopyrite structure. There has also been much recent interest in upgrading the copper content of concentrates. As such approaches involve changes in mineralogy, these are described in more detail in Part 2 [35].

The current development of a process by Orway Metallurgical Consultants for upgrading copper contents of concentrates for smelter feeds [36] is also relevant to this study, as this employs a combination of oxidative and non-oxidative hydrometallurgical process steps to drive metathetic alteration of the concentrate. A related approach was described by Fomenko et al. [37], who examined the effect of non-oxidative versus oxidative pre-treatment upon hydrothermal alteration of a copper-lead-zinc concentrate. The fundamentals of the non-oxidative upgrading of chalcopyrite have also been investigated using in situ XRD by Chaudhari et al. [38].

The application of various pressure oxidation technologies at the batch scale to processing a single chalcopyrite concentrate has been reported by this group [39,40]. These studies demonstrated the potential applicability of a wide range of processing conditions at temperatures between 100 and 220 °C, the beneficial effects of dissolved chloride, and the need for additives to prevent sulphur occlusion of the mineral surface at medium temperatures (120–160 °C). Although not specifically indicated, there was also an implication that the oxidation potential of the system can have a significant effect on the extent of leaching. This was suggested earlier in the study by Hackl et al. [41] of chalcopyrite leaching, employing a high-oxygen partial pressure (1380 kPa), in which low copper extractions were obtained even after prolonged leaching. In comparison, it has been demonstrated by employing a low-oxygen partial pressure that aggregate formation can be prevented or at least reduced [42], even in the absence of added sulphur dispersion agents [40]. Related to these investigations, several electrochemical studies note that the oxidative behaviour of chalcopyrite is significantly affected by the system potential [43–46]. An optimum potential window for chalcopyrite leaching in acid chloride solutions with the presence of oxygen was indicated, where, at higher potentials, leaching slows and the system becomes passive [45]. Debernardi et al. [47] found, in a low-chloride-content system, that reducing the extent of ferric compound precipitation on the chalcopyrite surface did not have a significant impact on the copper extraction rate, and it has been proposed instead (e.g., [21,41,46,48,49]) that a CuS₂ passivation layer formed in the presence of chloride is responsible for the slowing

of leaching. Most recently, evidence for a copper-rich, iron-deficient layer, thought to be “covellite-like”, was proposed by Ren et al. [50] to inhibit chalcopyrite leaching.

Other than the application of the CESL and Platsol[®] processes, the leaching of sulphides including chalcopyrite, specifically in chloride-containing media, is described in several reviews [13,25,51,52]. The benefits of using concentrated cupric chloride solutions for leaching sulphide minerals were considered by Lundstrom et al. [53], while Senanayake [54] examined the underlying reasons for the chloride enhancement of copper sulphide leaching. The use of alternative oxidants such as MnO₂ in the presence of chloride is described by Torres et al. [55]. It is notable here that the reaction between the MnO₂ and chloride in acidic conditions generates chlorine gas, which acts as a secondary oxidant. In comparison, the study of Kowalczyk et al. [56] indicated that the synergistic effect of MnO₂ and chloride (1 M NaCl), when compared to MnO₂, upon copper extraction from chalcopyrite (and isocubanite) resulted in an increased reaction rate and higher copper extraction.

The beneficial effects of chloride on chalcopyrite leaching have been known for many decades and are encapsulated by works such as those of Muñoz-Ribadeneira and Gombert [57] and Subramanian and Ferrajuolo [58], and direct leaching of chalcopyrite with ferric chloride can be traced back to Sullivan [59]. The effects of using chloride are attributed to several well-documented conclusions:

- The rate of leaching is enhanced (e.g., [60–66]).
- The rate of leaching is initially high (e.g., [66]).
- This rate becomes independent of the chloride concentration above a certain value (e.g., [64,67,68]).
- Enhancement occurs via the formation of chloride complexes (e.g., [51,66,68]), and more specifically, those of copper (I) [69].
- The formation of a compact layer of (solid) sulphur at the surface of particles that would slow down leaching is not found (e.g., [64–66]).
- Rather, a porous layer of sulphur is formed in the presence of chloride (e.g., [62,67,68]).

Most of experiments for this study were conducted over a decade ago. The focus on the examination of a process water types, and specifically those containing chloride ions, derived from noting the range of site water compositions encountered in Western Australia and their impact on nickel laterite ore processing (e.g., [70]). Since then, mounting pressure on the availability of potable water has resulted in mineral processors examining the impacts of alternative water supplies. Relevant examples here include the incorporation of seawater into the CESL process [71], while there is a significant body of work considering seawater use in processing Chilean copper ores ([72] and references therein).

In a previous study from this laboratory, it was noted that elemental sulphur can form and persist at high temperatures (220 °C) even though near-quantitative copper extraction had been achieved, when sodium chloride is added to the system [39]. The present studies were conducted to (re)examine the (batch processing) effects of various chloride-containing process fluids upon sulphur formation, which in turn delays complete oxidation, and methods for mitigating this behaviour. This first part of the study describes the leaching behaviour of chalcopyrite, with a focus on the effects of chloride in the process liquor. The impacts of other additives upon copper leaching are also considered. Part 2 examines the mineralogical characterisation of residue materials and correlations between the process fluid composition and changes in solids’ composition brought about in the presence of the various additives.

2. Experimental

A chalcopyrite concentrate (as received) was lightly ground and dry-screened to produce a $-45\ \mu\text{m}$ size fraction, employed as the feed material in most leaching experiments. Leaching was performed using a Parr 1 gal. (U.S.) 4551 M model vertical reactor (Parr Instrument Company, Moline, IL, USA), constructed from Grade 3 titanium, and controlled to within $\pm 2\ ^\circ\text{C}$ using a Parr 4842 model temperature controller. Agitation at speeds up to ca. 1000 rpm was provided by a magnetically driven twin-pitched blade impeller. Several studies have indicated that agitation at speeds above 600–700 rpm is enough to obtain good oxygen mass transfer (e.g., [73,74]), albeit somewhat dependent upon the type of batch vessel employed. Typically, the vessel was loaded with $\sim 2\ \text{L}$ of 10% or 20% *w/w* pulp density chalcopyrite concentrate slurry, with process fluids containing various dissolved salts and sulphuric acid at selected concentrations. The sealed autoclave was heated under a blanket of nitrogen to the required temperature, and oxygen was then injected on a continuous basis to maintain the target oxygen partial pressure and the reaction continued for 90 min. The experimental conditions are summarised in Table 1.

Table 1. Experiments conducted to examine the impact of chloride upon high-temperature pressure oxidation of chalcopyrite concentrate.

Pulp Density (% <i>w/w</i>)	Acid (g/L)	Chloride (g/L)	Additive(s)	T (°C)	P(O ₂) (kPa)
10	Nil	Nil	None	220	700
10 *	Nil	Nil	None	220	700
10	Nil	15	NaCl	220	700
20	Nil	Nil	None	220	700
20	30	Nil	None	220	700
20	100	Nil	None	220	700
20	Nil	3	NaCl	220	700
20	Nil	15	NaCl	220	700
20	Nil	15	NaCl, hematite seed	220	700
20	30	15	NaCl	220	700
20	Nil	15	NaCl	230	700
20	Nil	15	NaCl	245	700
20	Nil	15	NaCl	220	100
20	Nil	15	CuCl ₂ ·2H ₂ O	220	700
20	Nil	15	NaCl, Al ₂ (SO ₄) ₃ ·18H ₂ O #	220	700
20	Nil	15	NaCl, Gibbsite #	220	700
20	Nil	100	NaCl	220	700
20	100	100	NaCl	220	700
20	Nil	Nil	Na ₂ SO ₄ **	220	700

* Test conducted with $-75\ \mu\text{m}$ fraction. ** Sodium concentration was 2.8 M, the same as for the 100 g/L chloride addition as NaCl. # Amounts added were targeted to double the aluminium content in the system.

Samples taken at regular intervals from the autoclave were filtered through a $0.45\ \mu\text{m}$ Supor membrane, the primary filtrate was collected, and the solution density was measured using an Anton Parr DMA 35n density meter (Anton Paar GmbH, Graz, Austria). Solids were thoroughly washed with de-ionised water, dried overnight at $70\ ^\circ\text{C}$, and lightly ground. Both the liquor and solid samples were analysed by ICP-OES using either Varian Liberty 220 or Vista Pro instruments (Varian, Palo Alto, CA, USA) for the elements Cu, Fe, S, Si, Mg, Al, Ca, and Na. The residues were analysed after fusion at $900\text{--}1000\ ^\circ\text{C}$ with the Sigma Chemicals 12:22 lithium borate flux and dissolution. When sulphide and/or

elemental sulphur was present in the solids, sulphur analyses were performed using a LabFit CS-2000 analyser (LabFit Pty Ltd., Perth, Australia), with an electrical furnace heated to 1400 °C.

The acidity of filtrate samples was determined after dilution, with addition of a 20% excess of calcium EDTA solution and titration with sodium hydroxide, either to an endpoint pH of 5.7 or, for more recent results, the endpoint was determined from the inflection point of the titration curve using a 906 Titrando titrator in conjunction with Tiamo™ software (Metrohm AG, Herisau, Switzerland).

3. Ore Characterization

Quantitative X-ray diffraction (QXRD) analysis of the concentrate employed in the present study [35] indicated that the material consists of 71% chalcopyrite (CuFeS₂), 11% quartz (SiO₂), 7% pyrite (FeS₂), 8% talc (Mg₃(Si₂O₅)(OH)₄), 1.5% clinocllore (e.g., (Mg,Fe)₅Al(Si₃Al)O₁₀(OH)₈), and a trace amount of elemental sulphur. The calculated elemental analysis based on QXRD analysis was in excellent agreement with the chemical analysis obtained using ICP-OES and LabFit instruments. These data are presented in Table 2.

Table 2. Analytical data for the chalcopyrite concentrate.

Elemental Content (% w/w)							
Cu	Fe	Al	Mg	Ca	Si	Na	S
24.5	26.9	0.240	1.14	0.015	4.35	0.008	31.4

4. Background

4.1. Eh-pH and Eh-log[Cl⁻] Diagrams

According to the Eh-pH diagram for the Cu-Fe-S-H₂O system at 25 °C presented by Peters [75], and reproduced in Figure 1, a relatively low oxidation potential that decreases with increasing pH enables chalcopyrite conversion into various secondary copper sulphides (including bornite, chalcocite, and covellite), while pyrite is predicted to be stable during these transformations. The diagram indicates that sulphur can be oxidised to sulphate with a further increase in the oxidation potential, and that copper and iron remain dissolve under sufficiently acidic conditions. Iron when oxidised to the ferric form is unstable and hydrolyses to form hematite at relatively low pH values. Peters [76] noted, however, that in practice, sulphur is not oxidised to sulphate, except at sufficiently high overpotentials.

Senanayake [54] presented the Eh-log[Cl⁻] and Eh-pH diagrams for the Cu-Fe-Cl-H₂O and Cu-Cl-S-H₂O systems, respectively. Apart from changes in iron and copper speciation, the Eh-log[Cl⁻] diagram in particular indicates increasing stabilisation of copper (I) with the increasing chloride concentration. The Eh-pH diagram constructed specifically to indicate the stability of covellite and chalcocite indicates covellite dissolution above 600 mV (SHE) to form dissolved copper (II) species, atacamite (Cu₂Cl(OH)₃) or tenorite (CuO), depending on the pH. In non-chloride systems, basic copper sulphates that include antlerite (Cu₃SO₄(OH)₄) and brochantite (Cu₄SO₄(OH)₆) are predicted to form [77]. The formations of atacamite (or related basic copper chloride), antlerite, and brochantite have been found to occur under mild chalcopyrite pressure oxidation conditions (e.g., [40,78]), specifically when the extent of sulphur oxidation to sulphuric acid is low.

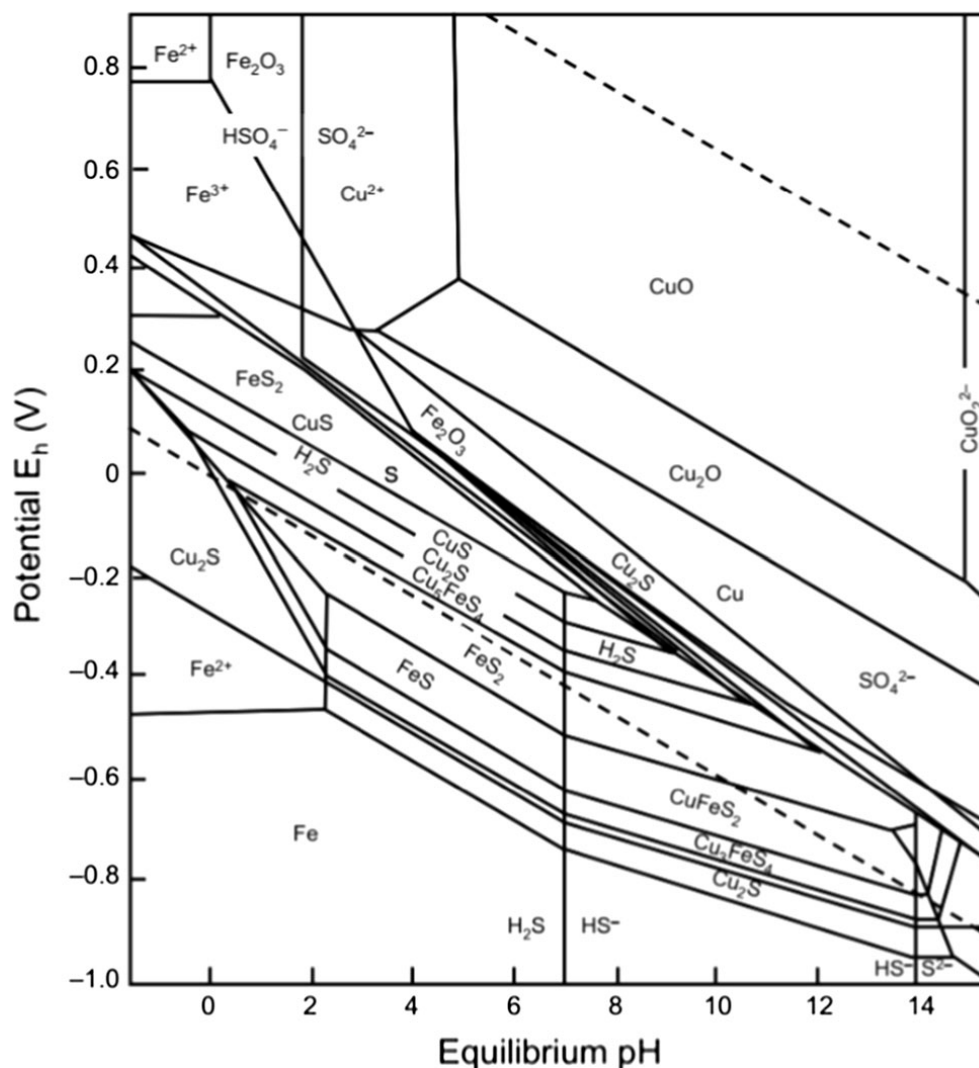


Figure 1. Pourbaix diagram for the Cu–Fe–S–O–H₂O system at 25 °C, [Cu] = 0.01 M, [Fe] = [S] = 0.1 M. Reproduced from Peters [75] (<https://doi.org/10.1007/BF02698582>, accessed on 15 June 2023). Potentials are relative to the standard hydrogen electrode (SHE).

4.2. Copper Sulphides' Extraction and the Effect of Eh

Velásquez-Yévenes et al. [79] proposed an optimum potential range for chalcopyrite dissolution in chloride solutions of 560–600 mV (SHE). Covellite and chalcocite formation, as intermediate phases, occurs at potentials below 550 mV. Yoo et al. [69] reported the optimum leaching rate for chalcopyrite in 0.1 M HCl and 0.1 M HCl plus 0.1 M H₂SO₄ to lie in the range 635–645 mV, while Jafari et al. [80] reported a range of 610–630 mV for chalcopyrite dissolution both without and with NaCl addition. The optimum redox potential window for acidic sulphate chalcopyrite leaching (in the presence of pyrite) determined by Koleini et al. [81] was 610–640 mV. Finally, an optimum redox potential for chalcopyrite dissolution in a non-chloride-containing environment that takes the initial Fe²⁺ and Cu²⁺ concentrations into consideration was also determined by Hiroyoshi et al. [82].

The dissolution of synthetic copper sulphides, covellite, chalcocite, and digenite, under conditions of controlled potential in the presence of chloride ions (added as 0.2 to 2.5 M NaCl), or hydrochloric acid (0.1 to 1 M), was studied by Miki et al. [83]. Conversion of digenite and chalcocite to covellite was demonstrated at a potential of 500 mV, while covellite started to dissolve when the potential was raised to 550 mV, and more preferably, 600 mV. The covellite dissolution rate was largely independent of chloride and hydrochloric acid concentrations. This agreed with the observations of Cheng and Lawson [84], who

reported that the rate increased with the increasing chloride concentration up to 0.25 M, above which the rate became independent of the chloride concentration to 2 M in the presence of 0.5 M sulphuric acid. Two-stage oxidation of chalcopyrite concentrate in 1 M sulphuric acid at 90 °C was noted to occur by Kametani and Aoki [85]. Specifically, when the solution potential was low (545–575 mV), the leaching of copper relative to iron was low due to the covellite formation. Below 675 mV, chalcopyrite was oxidised, while above 695 mV, pyrite was also dissolved.

In comparing chalcopyrite with covellite dissolution in chloride solutions, Nicol et al. [46] concluded that similar mechanisms applied to both or that covellite may be an intermediate in the dissolution of chalcopyrite. Like covellite, an increase of the chloride concentration by the addition of NaCl to 0.2 M HCl does not increase chalcopyrite dissolution [79]. That covellite is an intermediate in chalcopyrite dissolution is a conclusion also reached in the present study, and this is discussed in greater detail in Part 2 [35].

4.3. Surface Passivation of Chalcopyrite

The development of passivating layers on chalcopyrite has been studied by many groups and includes surface speciation (e.g., [86]) and electrochemical characterization (e.g., [43,87,88]) studies. These researchers demonstrated that the composition of surface layers and species present can vary as a function of several parameters, that include temperature, solution composition, leaching time, and oxidation potential, all of which are strongly interlinked. As comparative electrochemical studies, those of Liu et al. [49] and Lu et al. [65] are perhaps most informative in indicating, even when a passivating layer forms on the surface of chalcopyrite, that in the presence of chloride ions, this layer is much less protective. Since leaching is generally rapid at the temperatures employed in this study, it was concluded that passive layer formation may only be important during early stages of leaching, i.e., the first few minutes, when dissolved iron and copper levels are low, and/or the concentration of dissolved oxygen to drive the oxidation of Fe(II) and Cu(I) species is also low.

5. Results

5.1. Copper Extraction during Batch Processing

5.1.1. Effects of Chloride Addition, Pulp Density, and Particle Size

The major aim of this study was to develop insights into how changes in the process liquor composition impact upon the achievement of high copper extractions, not to demonstrate that high copper extractions could be obtained. Clearly, from examination of Figures 2 and 3, high extractions were obtained in less than 45 min, though the initial copper extraction rates were strongly impacted by the composition of the process fluid and pulp density. When de-ionised process water was employed, the extraction of copper was virtually complete within 10 min at a lower pulp density (10% *w/w*), but was much slower at a higher pulp density (20% *w/w*), taking just over 30 min. Additionally, when the particle size of the feed was larger ($P_{100} = 75 \mu\text{m}$), the extraction of copper at a pulp density of 10% *w/w* was marginally slower, but virtually complete after 20 min (Figure 2). The slowing of the reaction at a higher pulp density suggests that the reaction rate becomes increasingly limited by the diffusion of oxidant(s) to, and/or regeneration of oxidant(s) at, the chalcopyrite surface. It may also indicate that a more passive mineral surface develops during the early stages of the reaction.

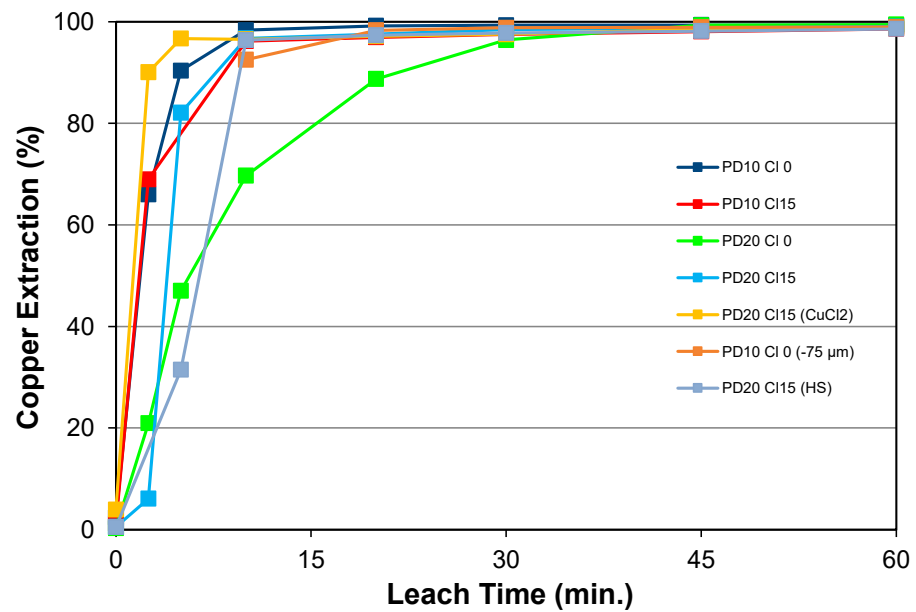


Figure 2. Extractions of copper from chalcopyrite concentrate (mostly $P_{100} -45 \mu\text{m}$) under pressure oxidation conditions ($220 \text{ }^\circ\text{C}$, 700 kPa O_2) at various concentrate pulp densities (PD as % w/w) and chloride (Cl as g/L) concentrations. Chloride was generally added as NaCl, except for in one test when it was added as $\text{CuCl}_2 \cdot 2\text{H}_2\text{O}$. A test for which the total pulp density was increased to 26.8% by hematite seed (HS) addition is also included.

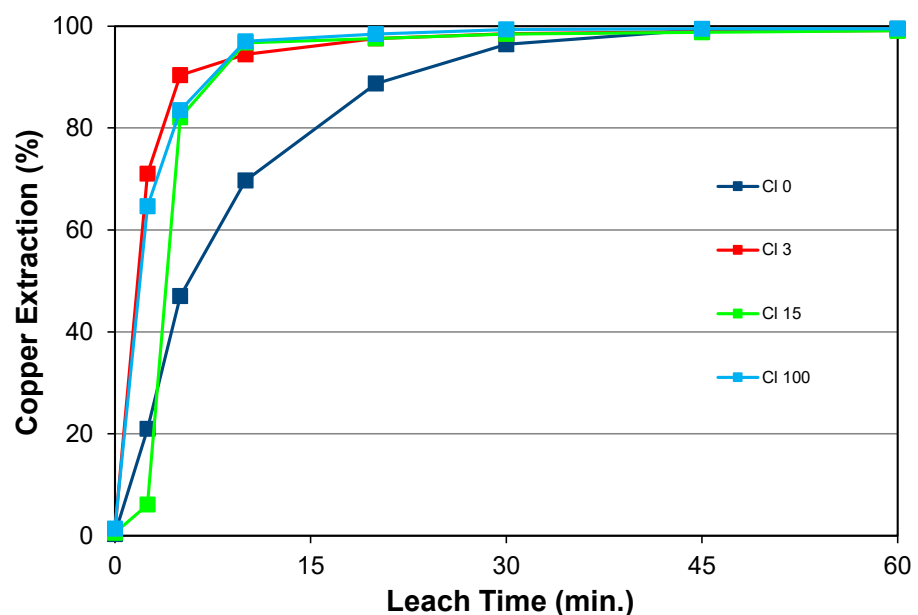


Figure 3. Extractions of copper from chalcopyrite concentrate ($P_{100} -45 \mu\text{m}$) under pressure oxidation conditions ($220 \text{ }^\circ\text{C}$, pulp density 20% w/w , 700 kPa O_2) at various chloride (Cl as g/L) concentrations. Chloride was added as NaCl.

A single test, for which the (total) pulp density was increased by hematite seeding to 26.8%, further confirmed the slowing of the initial reaction rate with the increasing solids' loading; though here, the diffusion of reactants to, and products from, the chalcopyrite surface are expected to have the main impact on the reaction rate.

In the presence of added chloride, and here the lowest addition employed was 3 g/L (i.e., 0.08 M), the initial rate of copper extraction was rapid (Figures 2 and 3). At higher chloride concentrations, extraction within the first 5 min was also rapid, but there was

virtually no difference between chloride additions of 15 g/L and 100 g/L. These data agree with the study of Lu et al. [64], who reported that increasing chloride concentrations above 0.5 M did not enhance the extraction rate at 95 °C. Muñoz-Ribadeneira and Gomberg [57] reported a similar outcome for extraction at low temperatures (25–35 °C). Ruiz et al. [89] reported that the chalcopyrite leaching rate did not increase above 0.5 M chloride at 100 °C, though this study did not examine chloride additions up to 0.5 M. In comparison, Qiu et al. [90] reported that for chalcopyrite leaching at 110 °C in the presence of chloride, the leaching rate starts to level off for NaCl concentrations of 60–70 g/L, i.e., 36–42 g/L (or above 1 M) of chloride. Similarly, Palmer et al. [67] reported, for leaching tests up to 96 °C, that the rate of chalcopyrite dissolution was independent of chloride concentration (added as NaCl, FeCl₃, or HCl, and mixtures thereof) above 1 M. Hence, based upon previous studies, there is clearly a chloride addition beyond which the rate of copper extraction is not enhanced, though what this level is at higher temperatures was not determined in the present study. Notwithstanding, the results indicate that process water composed of either seawater or reverse osmosis concentrate will be similarly effective in enhancing the extraction of copper from chalcopyrite under high-temperature pressure oxidation conditions.

It was noted that the addition of chloride as cupric chloride resulted in a faster initial extraction compared to NaCl addition (Figure 2), and this is consistent with a body of literature that describes the enhancement by cupric chloride on leaching kinetics at lower temperatures (e.g., [91]). Faster leaching in the presence of chlorides is consistent with the formation of (basic) chloride complexes at the chalcopyrite surface [54] that facilitate electron transfer between dissolved and solid-state ions.

When cupric chloride was added, extraction took longer to reach its maximum value (Figure 2). Notwithstanding that the reaction of copper (II) ions with chalcopyrite can form covellite under non-oxidising conditions, this may also indicate that diffusion of copper into the pyrite structure is better facilitated by the high starting copper concentration, and it is not until this mineral was fully oxidised that the additional copper reacting with the pyrite was recovered. The reaction of dissolved copper, both Cu(I) and Cu(II), with pyrite at high temperatures and the new mineral phases that can form have been described elsewhere (e.g., [92,93]).

At a higher pulp density (Figure 3), initial oxidation during the first 2.5 min released a small amount of copper and resulted mainly in the formation of intermediate covellite and hematite [35]. Thereafter, the rate rapidly increased, indicating that the dissolved oxygen content had sufficiently increased to sustain the reaction. In this case, the copper (I)/copper (II) oxidation-reduction couple drives the leaching, with oxygen primarily serving to cycle the dissolved copper species [54], as also noted for the digenite leaching [94]. Much earlier, Peters [95] also concluded that oxidation of a reduced species (e.g., Cu(I) and/or Fe(II)) to generate a surrogate oxidant drives the reaction, and that direct reaction between molecular oxygen and sulphide minerals is not significant. In more recent studies, it was concluded that while only a small fraction of the oxygen is incorporated in sulphate during the oxidation of pyrite [96], adsorption of molecular oxygen onto the pyrite surface plays a critical role in the mechanism of sulphate formation [97,98]. Certainly, if there are insufficient oxidising species present at the chalcopyrite surface, e.g., if cupric chloride species are removed by agitation, the reaction is slower [99].

In comparison to the current results, kinetic data for the Platsol[®] process indicated rapid leaching of copper (and nickel) sulphides within the first of six compartments, i.e., the first 20 min, during pilot-scale autoclave operation at 225 °C with 700 kPa oxygen overpressure [100]. Chloride is added as NaCl, typically 3–12 g/L Cl⁻, to complex precious metals, e.g., Ag/Au and PGMs [101]. Clearly, it also facilitated the leaching of chalcopyrite under these conditions.

Similarly, the application of brines containing 400 g/L MgCl₂ (i.e., ~300 g/L Cl⁻) to Ferguson Lake's massive sulphide ore, with 150% stoichiometric FeCl₃ relative to the sulphide content, were effective for the extraction of copper (from chalcopyrite) after a

prior leaching step to remove pyrrhotite and increase the Cu content of the treated solids to 3.6–5.1% [102]. Although leaching at 105 °C for 6 h with 5% *w/w* solids resulted in more than 98% copper extraction, increasing the temperature to 118 °C, near the brine boiling point, enhanced extraction to 97.9% after 2 h, and subsequently, to 99.8% after 6 h.

5.1.2. Effects of Acid Addition and Chloride

The upfront addition of acid at a 20% *w/w* concentrate pulp density was investigated primarily to examine the effect on the residue composition. However, as recycling of acidic raffinate from the copper SX circuit into the pressure oxidation step may be employed to close the water balance (e.g., [103–105]), acid addition to the leaching step is expected in a commercial application. Like the addition of chloride, it was also found that acid addition influenced copper extraction kinetics, as shown in Figure 4. Although not impacting the final copper extraction, the data suggest that increasing the initial acid concentration slows the overall leaching rate. This could indicate that the reacting chalcopyrite surface layers are more passive in nature, though it is noted that Córdoba et al. [21] also found slower leaching rates at a lower pH and concluded this could be explained if the $\text{Fe}(\text{SO}_4)_2^-$ species was primarily responsible for oxidation at the chalcopyrite surface. The formation of a copper-rich surface layer that is enhanced by increasing the sulphuric acid concentration is consistent with the conclusions of Hackl et al. [41] and Antonijević and Bogdanović [106], among others (Section 4.3). Similarly, Abraitis et al. [107] found that a copper- and sulphur-rich surface layer was formed, accompanied by net acid consumption. In the absence of oxygen, the following general reaction has been proposed for the formation of such a layer:

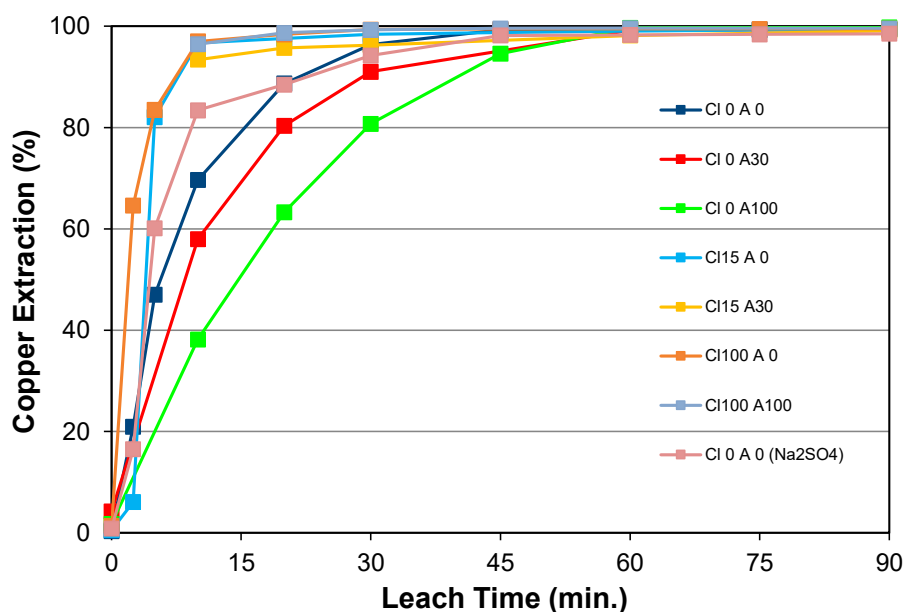
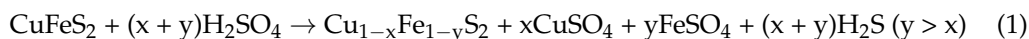


Figure 4. Extractions of copper from chalcopyrite concentrate ($P_{100} - 45 \mu\text{m}$) under pressure oxidation conditions (220 °C, pulp density 20% *w/w*, 700 kPa O_2) at various chloride (Cl as g/L) and initial acid concentrations. Chloride was added as NaCl and acid as H_2SO_4 .

Harmer et al. [86] also proposed that the composition of surface layers, and specifically the Cu-to-Fe ratio, which ultimately tends towards unity, evolves with time, where their model also includes the formation of elemental sulphur. The formation of a CuS_2 passivation layer has been proposed by others, as noted previously. This topic was recently revisited by Ren et al. [50], who suggested that since the leaching of covellite was similar to that of chalcopyrite, the surface layer is “covellite-like”. The formation of a passivation layer during the dissolution of covellite, however, has been proposed by Fu et al. [108] and

Nicol and Basson [109], the latter in chloride solutions, that were indicated to have Cu_4S_{11} and CuS_2 compositions, respectively. Finally, the generation of H_2S via the reaction of sulphuric acid with chalcopyrite under non-oxidising conditions, e.g., during the heating period of the current experiments, was demonstrated in the study of Recalde Chiluiza and Navarro Donoso [110].

The initial preferential leaching of iron was reflected in the dissolved iron levels prior to oxygen injection in the current study: 2.1–2.5 g/L for no acid addition, 6.9–8.2 g/L for 30 g/L acid addition, and 8.6–13.0 g/L for 100 g/L acid addition. The dissolved copper levels were always lower than the dissolved iron levels with upfront acid addition, ranging from 0.7–2.9 and 0.4–1.2 g/L for 30 g/L and 100 g/L acid additions, respectively. As found previously, for the absence of upfront acid addition (see Figure 3), the addition of chloride with acid enhanced the leaching rate, enabling near complete leaching to occur between 10 and 20 min (Figure 4). It was notable that for the 15 g/L chloride addition with 30 g/L of acid, copper extraction was marginally lower than with no acid addition, and the residual fraction of copper remaining after 10 min slowly leached thereafter. This suggests that a somewhat more passive surface was maintained under these conditions.

5.1.3. Effect of Temperature with Chloride Addition

The effect of temperature upon copper extraction was most noticeable during the first 10 min, as shown in Figure 5; thereafter, extraction only marginally increased. The slower initial extraction during the first 2.5 min (measured only at 220 °C and 245 °C) is expected to be reflective of batch conditions for which oxygen injection enables system Eh to be increased to a stable value a short time after the reaction commences. During this time, less oxidising conditions will result in reactions occurring that may differ from the primary reaction(s) expected.

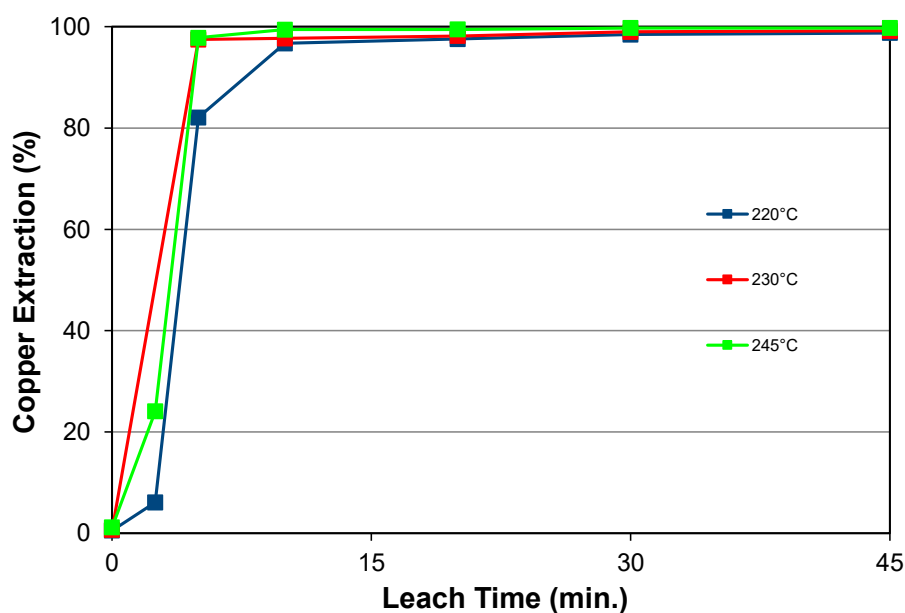


Figure 5. Extractions of copper from chalcopyrite concentrate ($P_{100} - 45 \mu\text{m}$) at various temperatures under pressure oxidation conditions (pulp density 20% w/w , 700 kPa O_2) with 15 g/L of chloride added as NaCl.

5.1.4. Effect of Oxygen Pressure

The reaction order with respect to oxygen partial pressure for pressure oxidation of pyrite at temperatures between 140 and 180 °C has been reported to be 1 [111]. For chalcopyrite, Yu et al. [112] determined the temperature dependence between 125 and

175 °C for the rate of chalcopyrite leaching, K , using a simple shrinking-core model, as a function of oxygen partial pressure, PO_2 :

$$K = \frac{A PO_2}{1 + B PO_2} \quad (2)$$

Here, A and B are temperature-dependent constants, and the rate is approximately linear for lower oxygen partial pressures, similar to the range used in this study (100–700 kPa), approaching a limiting value at higher oxygen partial pressures. Based on the values given for A and B [112], increasing the temperature results in the relative reaction rate for oxygen partial pressure of 700 kPa to that for a partial pressure of 100 kPa decreasing with the increasing temperature, from 7.0 to 6.2 between 125 and 175 °C.

In the present study, the extraction of copper is almost 99% after 10 min at both a low (100 kPa) and higher oxygen partial pressure (700 kPa), as shown in Figure 6, in both cases greater than when the solution contains no added NaCl. Thus, although a decrease in oxygen solubility is expected when NaCl is added [113], the faster copper extraction combined with the difference in the shape of the copper extraction curve are both consistent with the reaction mechanism differing in the presence of chloride, as discussed by Senanayake [54]. Furthermore, the studies of Tromans [114,115] concluded that the presence of additives at high temperatures has minimal impact on the oxygen mass transfer required for regeneration of the primary oxidant species. This is borne out by a comparison between systems containing no additive and Na₂SO₄ addition at equivalent molarity to the 100 g/L chloride addition as NaCl (Figure 6). A high sulphate concentration will also have an impact by buffering the acid produced, and will enable a higher concentration of the Fe(SO₄)₂⁻ species, proposed by Córdoba et al. [21] to be the primary oxidant in this system.

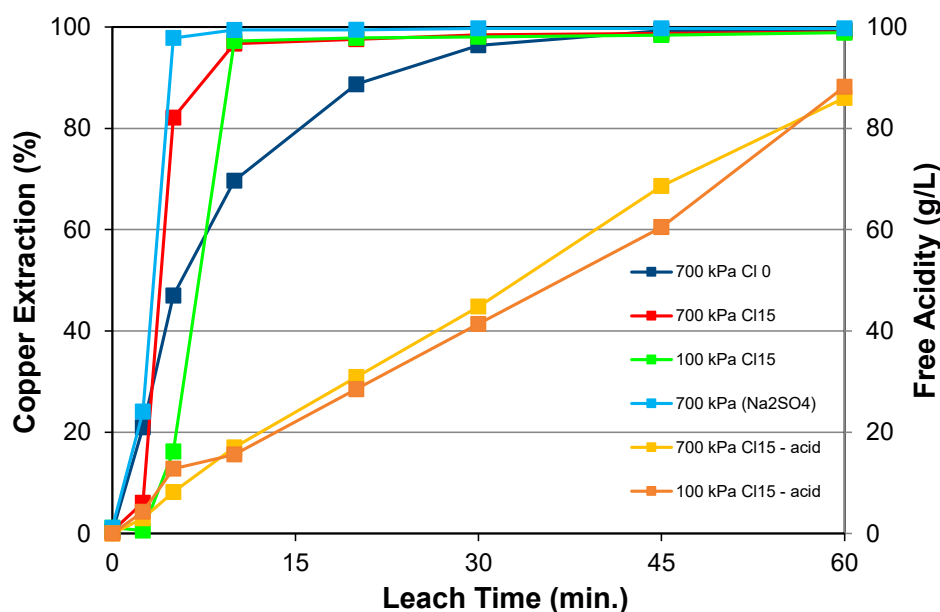


Figure 6. Extraction of copper from chalcopyrite concentrate ($P_{100} = 45 \mu\text{m}$) under pressure oxidation conditions (220 °C, pulp density 20% w/w , 15 g/L Cl) at different oxygen partial pressures (kPa). Chloride was added as NaCl. The curves when no NaCl was added and for the addition of 1.4 M Na₂SO₄ are presented for comparison.

Although the extraction of copper (and free acidity) is virtually identical from 10 min onward in the presence of chloride at different oxygen pressures (Figure 6), there is a clear impact of a lower oxygen pressure in decreasing the copper extraction rate up until that time. This is consistent with the formation of a covellite intermediate [35]. The generation of sulphuric acid (from elemental sulphur formed when chloride is present) from 10 min onwards occurs at similar rates, suggesting that this reaction does not have

a strong dependence upon oxygen partial pressure at 220 °C. The decoupling of copper extraction from sulphuric acid generation when chloride is present is discussed in the following sections.

5.2. Sulphuric Acid Addition and Formation

5.2.1. Effects of Pulp Density, Chloride Addition, and Temperature

The change to the rate of sulphuric acid formation in the presence of chloride during pressure oxidation of chalcopyrite at 220 °C has previously been reported [39]. A comparison of the free acid values for samples taken during selected experiments is presented in Figure 7.

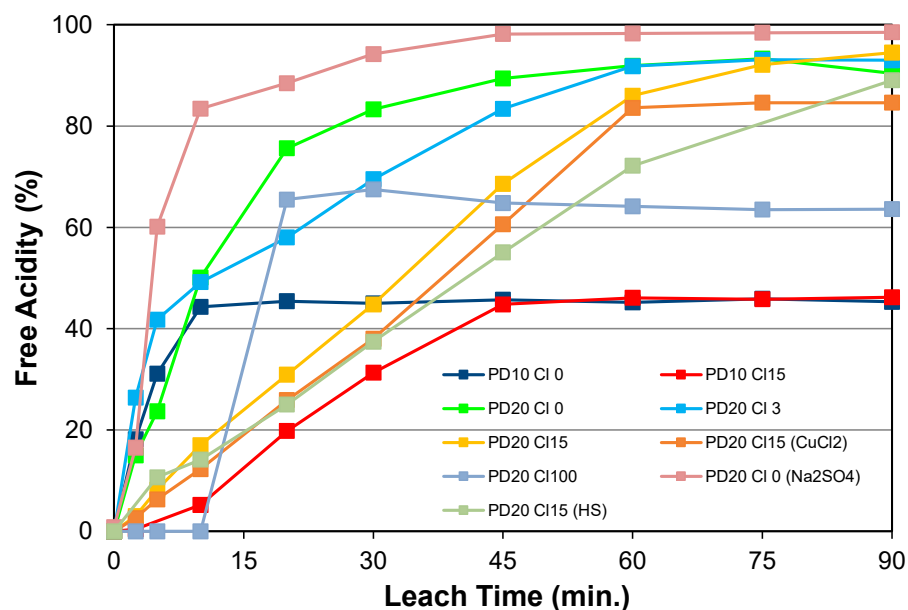
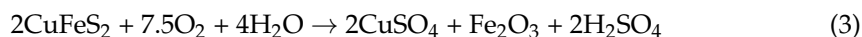


Figure 7. Change in free acid concentration during the leaching of chalcopyrite concentrate (P₁₀₀ –45 µm) under pressure oxidation conditions (220 °C, 700 kPa O₂) at various pulp densities (PD as % w/w) and chloride (Cl as g/L) concentrations. Chloride was generally added as NaCl, except when it was added as CuCl₂·2H₂O. The effects of adding Na₂SO₄ and hematite seed (HS) are shown for comparison.

At a low pulp density (10% w/w) and in the absence of chloride, the sulphuric acid concentration quickly rises, in parallel with copper extraction, and flattens out after ~10 min. This corresponds to rapid, total oxidation of sulphur and is supported by residue characterisation [35]. The equation describing these observations is:



In contrast, at a 10% w/w pulp density in the presence of chloride (15 g/L), the sulphuric acid concentration does not stabilise until after 45 min, although copper extraction is rapid, mostly occurring within the first 10 min (Figure 2). Examination of the leach residue indicates that this is due to incomplete oxidation and that elemental sulphur is present in the interim samples [35].

At a higher pulp density (20% w/w), sulphuric acid formation in the absence of chloride is more gradual, and again parallels copper extraction kinetics, e.g., Figure 2. In the presence of chloride, sulphur persists in the residues for longer, up to around 60 min, considering that more is produced than at the lower pulp density [35]. When chloride is added as cupric chloride salt, sulphuric acid formation parallels that found when added as NaCl. This implies that the presence of chloride controls the formation of elemental sulphur.

With a small addition of chloride (3 g/L), the data indicate a relatively fast initial production of sulphuric acid (due to iron hydrolysis) during the first five minutes, by

which time near-quantitative copper extraction is achieved (Figure 3). Thereafter, slower generation is primarily driven by the oxidation of elemental sulphur (and to a lesser extent, unreacted pyrite). With a moderate chloride addition (15 g/L), the initial production of sulphuric acid was slower, its concentration only becoming like that of the lower (and no) chloride systems at around 75 min. For a chloride concentration of 100 g/L, (net) sulphuric acid formation was strongly suppressed during the first 10 min, by which time copper extraction was around 96–97% (Figure 5). At this point, the solution was slightly acidic, with the free acidity below 1 g/L, though just over half of the sulphur reported to the solution as copper sulphate. Between 10 and 20 min of leaching in the presence of 100 g/L of chloride, sulphuric acid was rapidly produced, suggesting that the chloride concentration affects the rate of elemental sulphur oxidation. In contrast, at 200 °C, Corriou and Kikindai [116] indicated that the effects of increasing acid (HCl and H₂SO₄) and salt (NaCl and Na₂SO₄) concentrations were to decrease the rate of sulphur oxidation. It was concluded that this increase was not simply associated with elemental sulphur oxidation, as other reactions involving acid use and generation significantly contributed to the behaviour noted during the first 20 min. This is further discussed elsewhere [35], where it is reported that the stable acid concentration reached is consistent with the formation of a significant proportion of sodium jarosite. Notably, however, elemental sulphur did not persist in the leach residue for much longer than 30 min.

It is clear from the data presented that chloride addition affords separate control over the rates of both copper extraction and sulphide oxidation. Chalcopyrite is initially transformed to intermediate covellite, that is then leached, generating elemental sulphur, which is subsequently oxidised to sulphuric acid (also see [35]). Based on the mechanism proposed by Senanayake [54], the hypothesis is that surface complexation with chloride ions controls the rate of chalcopyrite transformation to covellite. While covellite is leached more rapidly than chalcopyrite [84], surface chloride complexation will further enhance copper dissolution. Since covellite leaching produces elemental sulphur that is subsequently oxidised and over a longer time, a greater proportion of the oxidant will be employed for copper dissolution.

The decoupling of copper extraction and sulphur oxidation could confer benefits to a high-temperature pressure oxidation process by reducing the oxygen requirements and yet still enabling high copper extraction through control of the oxygen partial pressure and/or residence time. Furthermore, there may be an opportunity to recover sulphur from the residue, while neutralisation costs for the leachate produced would also be reduced. Conversely, the lingering presence of elemental sulphur, as indicated by the lower free acid levels and residue mineralogy data [35], may be detrimental to downstream processing, e.g., when pressure oxidation is applied to materials that also contain economic quantities of gold [117]. It is well-known that elemental sulphur reacts with cyanide, leading to consumption of the latter during conventional cyanidation to recover gold [118].

It is notable that many plots of free acidity are essentially linear whenever elemental sulphur is present (Figure 7). Note that these linear regions do not necessarily correspond to when elemental sulphur is being oxidised, as sulphuric acid production is augmented by other reactions and may be quicker during rapid iron hydrolysis or slower if acid is consumed for mineral dissolution and/or iron oxidation [35]. In comparison, Habashi and Bauer [119] reported linear rates of oxidation for elemental sulphur at temperatures up to 170 °C, which would give rise to a linear increase in the acid concentration. Corriou and Kikindai [116] reported that the mean reaction rate between 125 and 230 °C is a fractional power function of sulphur mass, and that this function changes as the form of the sulphur changes, between 160 and 180 °C. The same authors also indicate that the mean rate of sulphur oxidation at 200 °C is of the same magnitude for both chloride- and sulphate-containing systems. In the present study, this implies that chloride primarily impacts upon the chalcopyrite oxidation mechanism, resulting in preferential formation of sulphur, rather than significantly impacting the sulphur oxidation rate. Copper extraction and sulphuric acid formation, as described previously, are also decoupled in the reaction mechanism, with

the former invariably exceeding the latter when chloride is present, as clearly shown by a plot of dissolved copper versus sulphur species concentration (Figure 8). Thus, leaching of the covellite intermediate formed in the presence of chloride [35] appears to follow the mechanism proposed by Ruiz et al. [94] for temperatures between 50 and 90 °C.

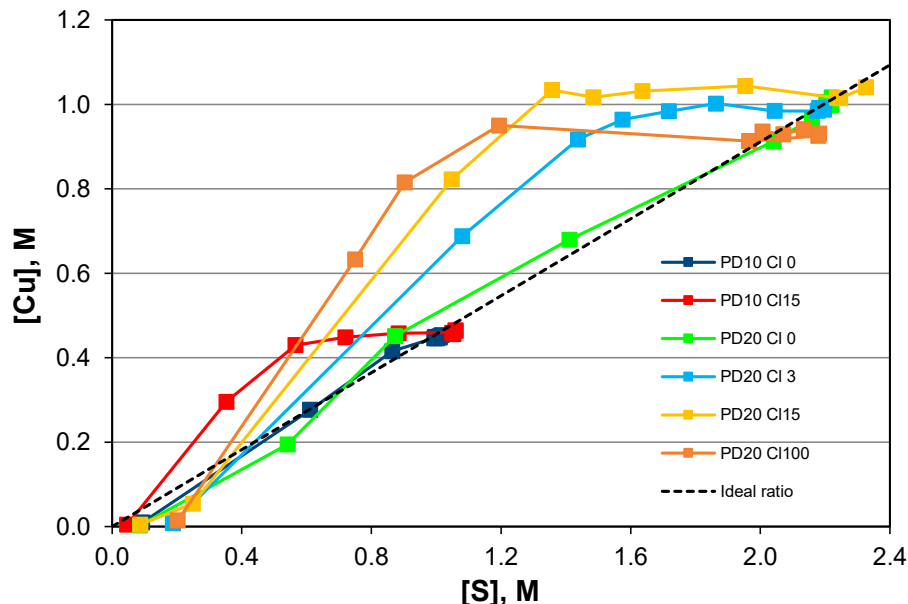
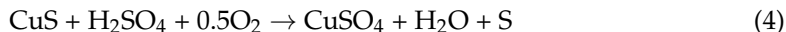


Figure 8. Change in dissolved copper versus sulphur-containing species concentrations during the leaching of chalcopyrite concentrate (P₁₀₀ –45 µm) under pressure oxidation conditions (220 °C, 700 kPa O₂) at various pulp densities (PD as % w/w) and chloride (Cl as g/L) concentrations. Chloride was added as NaCl. The dotted line represents the ratio of copper to sulphur in the concentrate.

Ghali et al. [120] also proposed that chloride accelerated the formation of sulphur during the electro-dissolution of chalcopyrite in hydrochloric acid. For this reaction, a source of acid is required, which must derive from the hydrolysis of iron, and hence, during the early stages of leaching while the acid concentration remains low, the overall reaction via covellite intermediate is given by:



This equation is consistent with the chemistry of the system when the chloride addition was 100 g/L, for which no covellite was found in samples taken once the pressure oxidation was commenced [35]. It may also simply indicate that any covellite intermediate formed had reacted within the first 2.5 min, the earliest a sample was taken once oxygen injection was commenced during this study.

The test with Na₂SO₄ addition of an equivalent sodium concentration to the addition of 100 g/L of chloride as NaCl (i.e., 2.8 M) indicated the most rapid generation of acid. Considering that the starting sulphate concentration was 145 g/L, this will strongly favour formation of the Fe(SO₄)₂⁻ species, which Córdoba et al. [21] suggested was primarily responsible for oxidation at the chalcopyrite surface in the sulphate system.

It is expected that sulphuric acid formation from elemental sulphur proceeds as per the overall equation:



This reaction was reported by Habashi and Bauer [119] to be catalysed by the presence of metal ions, such as Cu(II). Elemental sulphur hydrolysis in the absence of oxygen nominally generates sulphide in addition to sulphate [116,121,122], and hence, oxygen

is required, as shown by Habashi and Bauer [119], for complete (hydrothermal) sulphur oxidation, which is dependent upon the oxygen partial pressure. Furthermore, sulphide oxidation in minerals such as pyrite generates sulphate, for which most of the oxygen atoms derive from water [123]. A similar result was obtained by Reedy et al. [124], who performed ^{18}O tracer studies to conclude that the dominant (if not sole) oxidant was ferric iron; however, the possibility oxygen is involved as the initial oxidant could not be excluded. Usher et al. [125] suggested that oxygen atoms in the iron oxyhydroxide product formed during pyrite oxidation seem to derive from molecular oxygen. This implies that oxygen acts as an electron acceptor during oxidation of metal ions, being reduced to form various surface species [98,126,127]. A similar conclusion was reached for chalcopyrite oxidation [128] and is not contradicted by insights from a recent first-principles study [129].

Plots of the %S in solution as a function of time (Figure 9) are also informative, and these data complement the deportment of sulphur in the leach residues [35]. Note that the molar ratio of S:Cu in the concentrate is 2.1:1 due to the presence of a small amount (7%) of pyrite (see Section 3). In these tests, the oxidation of sulphur to soluble species (e.g., sulphate) provides an indication of how the leaching reactions proceed. The oxidation of sulphur is most rapid at a 10% *w/w* pulp density in the absence of chloride. In comparison, when chloride is present (15 g/L), increasing the temperature to 245 °C also enhances the rate of sulphur oxidation, though at the higher temperature, jarosite formation is favoured over hematite [35] and an increasing proportion of sulphur reports to the residue as the system tends toward equilibrium. Where significant amounts of sodium/hydronium jarosite are formed, the percentage of dissolved sulphur is lower or falls away as the reaction proceeds, e.g., when 100 g/L of chloride was added (as NaCl).

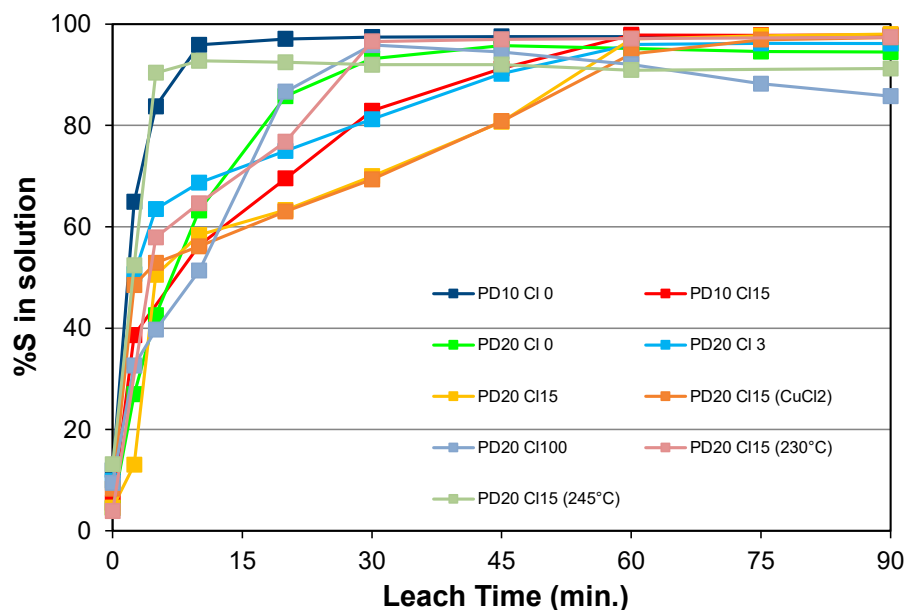


Figure 9. Change in dissolved sulphur-containing species concentrations during the leaching of chalcopyrite concentrate ($P_{100} - 45 \mu\text{m}$) under pressure oxidation conditions (700 kPa O_2) at various pulp densities (PD as % *w/w*), chloride (Cl as g/L) concentrations, and temperatures (220 °C, unless stated otherwise). Chloride was normally added as NaCl.

Many of the plots in Figure 9 where chloride is added have sections where dissolved sulphur linearly increases (or near so), and these correspond, as previously discussed, to oxidation of elemental sulphur in the system. When no chloride is present, the plots gradually increase toward the maximum value, and this corresponds with slower oxidation of sulphide minerals in the system to form sulphate (without intermediate sulphur formation). The data in the figure suggest that there is a concentration of chloride ions for which sulphate formation is hindered, and above which, the sulphur oxidation rate then

increases. Studies employing a range of reverse osmosis concentrates would be informative on this matter.

The reproducibility of free acid values from duplicate tests is shown in Figure 10. Although indicating differences in the absolute values, and this is expected to mainly derive from concentrate sub-sampling variation, the trends previously noted are the same, where increasing the addition of chloride up to 15 g/L slows sulphuric acid generation. For an addition of 100 g/L of chloride, rapid net acid generation occurs only after 10 min. Prior to this time, the acid generated by reactions such as the oxidation of elemental sulphur (Equation (6)) is consumed by the oxidation of chalcopyrite (Equation (5)). Hence, the basic copper chloride salt clinoatacamite ($\gamma\text{-Cu}_2(\text{OH})_3\text{Cl}$) was formed and detected in both the 2.5 and 5 min samples [35]. As the formation of this salt generates acid, this is expected to contribute to that required for the sustained oxidation of chalcopyrite during the first few minutes of the reaction.

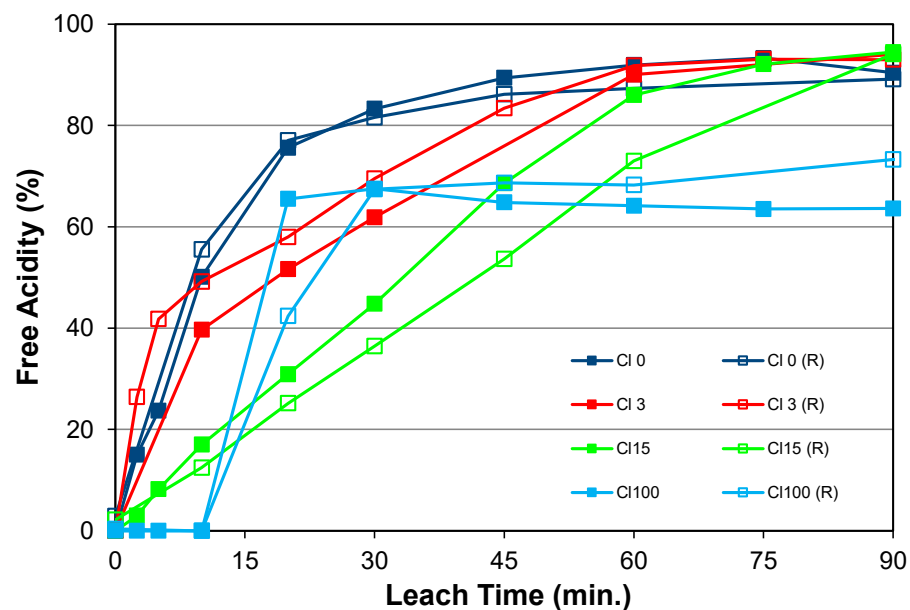
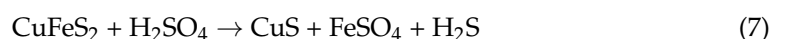


Figure 10. Change in free acid concentration during the leaching of chalcopyrite concentrate ($P_{100} - 45 \mu\text{m}$) under pressure oxidation conditions ($220 \text{ }^\circ\text{C}$, 700 kPa O_2 , pulp density $20\% w/w$) at various chloride (Cl as g/L) concentrations. Chloride was added as NaCl. R refers to a repeat set of data.

5.2.2. Effect of Initial Acid Addition

When acid was added to the pulp beforehand, some was consumed during the heat-up period. Examination of Figure 11 indicates that for acid additions of 30 and 100 g/L with no chloride, the free acidity had dropped in both cases by around 25 g/L before the oxygen injection commenced. In both cases, this corresponds to the preferential extraction of iron into solution (ca. 8 g/L), as already noted in Section 5.1.2, with the formation of a small amount of covellite [35]. A non-oxidative reaction of this kind can be simply written according to various researchers (e.g., [75,130]) as:



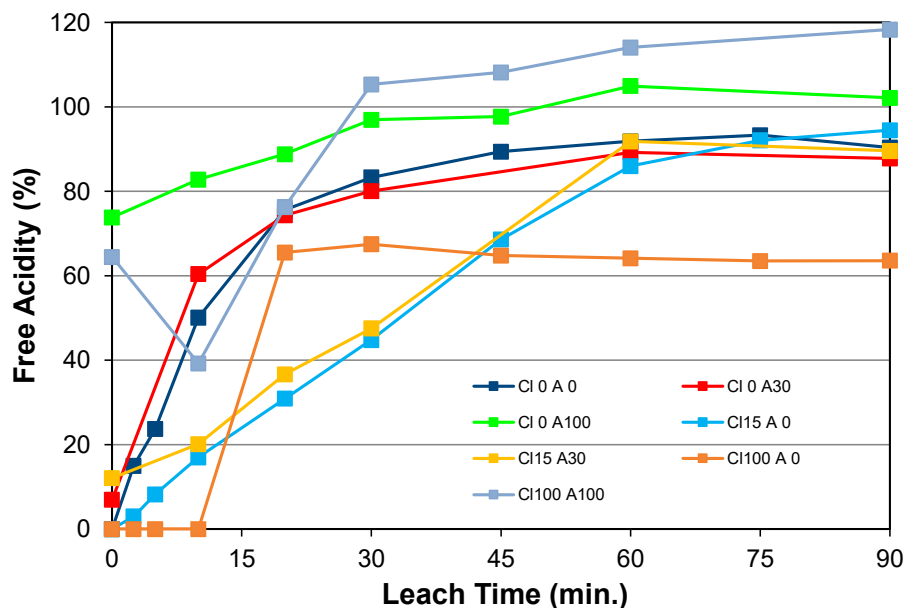


Figure 11. Change in free acid concentration during the leaching of chalcopyrite concentrate ($P_{100} - 45 \mu\text{m}$) under pressure oxidation conditions ($220 \text{ }^\circ\text{C}$, 700 kPa O_2 , $20\% w/w$ pulp density) at various chloride (Cl as g/L) and upfront sulphuric acid (A as g/L) concentrations. Chloride was added as NaCl.

That a small amount of copper (1.2 g/L) was also dissolved is consistent with the following net reaction occurring in parallel:



Although hydrogen sulphide can react with sulphuric acid [131,132] and with both ferric and cupric ions, elemental sulphur is expected to form. No crystalline sulphur, however, was detected in the t_0 samples [35]. This also suggests that H_2S has low solubility in the system, also as the odour of this gas emanating from the liquor samples was not noticeable.

Invariably, surface air oxidation of the chalcopyrite concentrate can occur upon ageing, and the presence of small amounts of metal sulphates that readily dissolve in water may have contributed to the copper and iron tenors prior to the commencement of oxidation. However, the bulk of the dissolved iron is expected to be represented as ferrous sulphate. Marsden et al. [27] reported that this material is deposited as scale during continuous chalcopyrite leaching at $215\text{--}230 \text{ }^\circ\text{C}$ if insufficient oxygen is available to completely oxidise iron.

In most instances, there was net acid generation as the reaction proceeded and where there was a sustained linear increase in concentration, and this has been largely ascribed to oxidation of elemental sulphur. For the addition of 100 g/L of chloride with an acid addition of 100 g/L , the free acidity initially dropped. This is due to a combination of sulphur formation, as given by Equation (5), which is net acid-neutral, and the formation of jarosite (which is net acid-consuming) instead of hematite [35]. The subsequent oxidation of elemental sulphur to 30 min followed by the slow decrease in the iron concentration resulted in the free acidity continuing to increase throughout this reaction. Although free acidity increased throughout the reaction with no chloride addition and acid addition of 100 g/L , the net increase was small compared to that for reactions with no acid addition. This indicates that a substantial proportion of the acid generated is associated with the phases in the residue, as discussed elsewhere [35].

5.3. Behaviour of Dissolved Iron

The leaching of iron associated with upfront sulphuric acid addition was previously discussed in Section 5.1.2. Figure 12 shows a comparison of the changes in iron concentrations during leaching for selected tests. First, the two sets of data obtained with no chloride addition demonstrated a small degree of experimental variation, where the final free acid concentrations differed by ~1 g/L. In both instances, it was clear that the equilibrium iron concentration had not been reached. The addition of 3 g/L and 15 g/L of chloride facilitated elemental sulphur formation, and therefore, the iron concentration only rose as oxidation of sulphur to sulphuric acid occurred. Although the final free acid concentrations were similar, the final iron concentrations significantly differed, suggesting that the rapid generation of sulphuric acid results in a significant deviation from the equilibrium state over the timeframe of these experiments. That said, data for the addition of 100 g/L of chloride were informative, showing iron concentrations dropping to near zero (~150 mg/L) after oxidation of the ferrous iron and hydrolysis, and only increasing after the elemental sulphur formed was oxidised to sulphuric acid. As there was a time lag before the net generation of significant free acidity (by 10–20 min), as shown in Figure 7, the acid formed during at least the first 10 min was primarily used to facilitate Fe(II) oxidation (and the dissolution of the clinoatacamite formed [35]). Subsequently, the iron concentration peaked, and thereafter decreased as the solid-solution equilibrium was approached. In comparison, when Na₂SO₄ was added, acid generation rapidly occurred from the start of the reaction (Figure 7), and a longer period where the iron concentration slowly decreased was noted. Furthermore, in situ buffering of the acidity by the high sulphate concentration (~325 g/L compared with typical values of 195–225 g/L) allowed a lower final iron concentration to be achieved, even though the final free acidity was high (99 g/L).

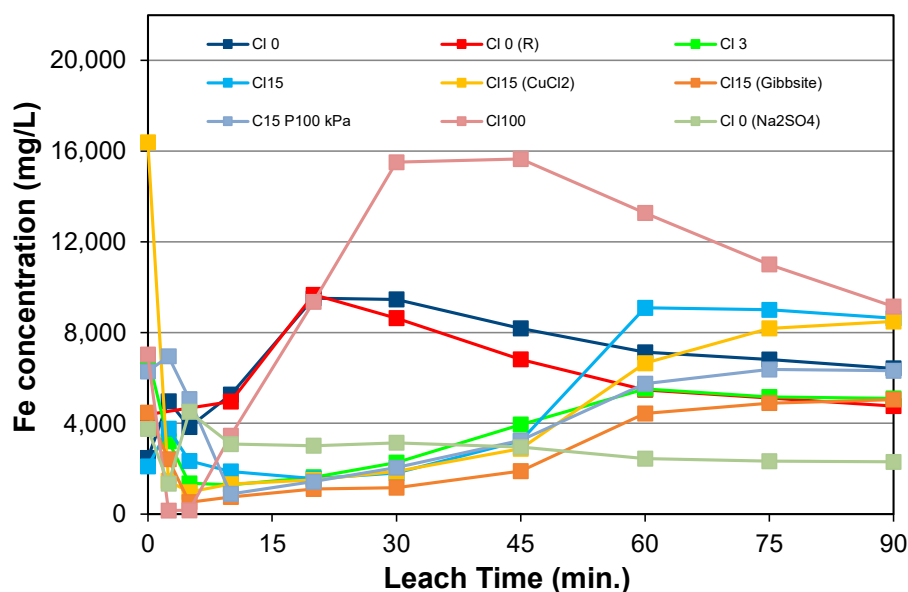


Figure 12. Changes in iron concentration during the leaching of chalcopyrite concentrate (P₁₀₀ –45 μm) under pressure oxidation conditions (220 °C, 20% w/w, 700 kPa O₂ except for test at 100 kPa) with no and various salt additions. Chloride was generally added as NaCl, except when it was added as CuCl₂·2H₂O. Other additives, including gibbsite and sodium sulphate, are noted. R refers to a repeat set of data.

As a larger number of tests were conducted with 15 g/L of chloride added, several datasets could be compared to look for a pattern of behaviour (see Figure 12). Each of these plots at times between 5 and 45 min indicate iron concentrations below 5 g/L, consistent with high rates of Fe(II) oxidation to Fe(III), compared to slower elemental sulphur oxidation rates. The increasing free acidity as sulphur oxidation became the

dominant oxidation process resulted in the iron solubility substantially increasing after 45 min, as previously discussed.

For chloride addition as $\text{CuCl}_2 \cdot 2\text{H}_2\text{O}$, 16.4 g/L of iron reported to the t_0 sample, i.e., prior to oxygen injection. This is consistent with iron being present primarily as Fe(II) (due to the rapid reaction between Cu(I) and Fe(III)), since Fe(III) solubility relative to hematite formation was low and only increased to ~2 g/L as free acidity increased to ~90 g/L, based on the data of Reid and Papangelakis [133]. For this sample, the dissolution of iron was also of similar magnitude on a molar basis to the loss of copper from liquor and symptomatic of metathetic conversion of chalcopyrite to covellite [35]. Commencement of the oxygen injection resulted in a rapid decrease in the iron concentration as it oxidised and hydrolysed to form hematite.

Several other observations can be made from Figure 12:

1. The iron concentrations during early leaching were somewhat higher when a lower oxygen partial pressure was employed, reflecting slower rates of sulphuric acid generation and Fe(II) oxidation.
2. As the dissolution of added gibbsite was net acid-consuming, the final free acidity was lower, and this corresponds to a lower final iron concentration.
3. The variation in final iron concentrations for the various datasets suggests that the equilibrium between the solids and liquor compositions was not reached after 90 min.

Since the presence of sulphur may be detrimental to downstream processing of the solids, the effect of temperature on the persistence of sulphur when chloride is present was investigated at higher temperatures for a chloride addition of 15 g/L, and the effect of temperature on copper extraction was discussed in Section 5.1.3. Iron concentration and free acidity data at the various temperatures are compared in Figure 13. First, as expected, the final iron concentration decreased with increasing temperature and was consistent with the decreasing solubility of hematite [134]. The delay in the maximum iron concentration being reached decreased between 220 and 230 °C and was essentially eliminated at 245 °C. This delay is consistent with the formation of elemental sulphur and its subsequent oxidation to sulphuric acid at lower temperatures. The peak in the iron concentration of 19.4 g/L at 245 °C indicates that the rate of iron oxidation (Equation (9)) is slower than that of sulphuric acid generation, considering that both ferrous iron and sulphuric acid concentrations were simultaneously increasing during the initial period of the reaction. It may also reflect a slower than required rate of oxygen mass transfer during this period to enable the following reaction:



Increasing the reaction temperature to 230 °C increased the rate at which elemental sulphur was oxidised, and therefore, the rate of sulphuric acid generation. At 245 °C, the rate of acid formation was fastest and coincided with the near absence of elemental sulphur in the leach residues. Furthermore, the lower final free acidity corresponds to the formation of natrojarosite that occurred from around 10 min, whereas at lower temperatures, little of this phase was formed. These changes to the leach residue mineralogy are discussed elsewhere [35].

Although there is some conjecture about the properties of sulphur at high temperatures, a temperature of 245 °C is close to the auto-ignition temperature reported for the surface of liquid sulphur to lie in the range 248–261 °C ([135], p. 42). This is consistent with little sulphur being found in the residues generated at 245 °C due to a rapid hydrothermal reaction.

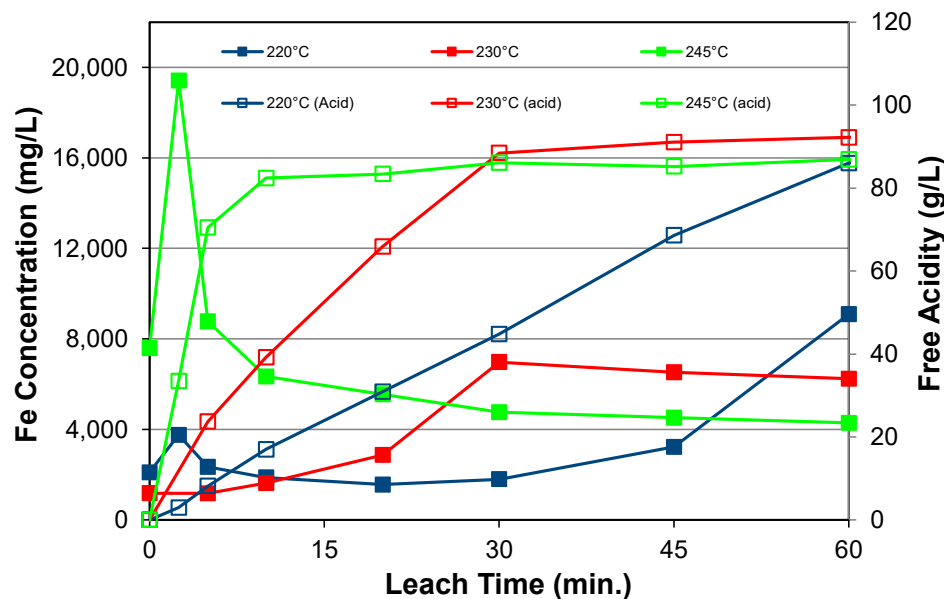


Figure 13. Changes in the iron concentration and free acidity during the leaching of chalcopyrite concentrate ($P_{100} - 45 \mu\text{m}$) under pressure oxidation conditions (20% w/w , PO_2 700 kPa) with a 15 g/L chloride addition (as NaCl) at various reaction temperatures.

5.4. Behaviour of Other Elements

The leach solutions generated contained low concentrations of other elements that typically fell within the following ranges for an experiment conducted using a 20% w/w pulp density feed: Al 500–1200 mg/L, Ca 400–500 mg/L, Mg 1200–2600 mg/L, and Si 400–500 mg/L. Generally, the concentrations increased with the reaction time for Al and Mg; for Si, the concentration was noted to peak in the range 650–700 mg/L, and subsequently drop over the remainder of the reaction, in some cases to around 100 mg/L. Calcium was mostly dissolved by the time the reaction commenced. Typically, the extractions of these impurity metals were in the following ranges: Al 55–75%, Ca > 95%, Mg 50–70%, and Si 3–4%. These and previous data are consistent with calcium being hosted by a mineral such as calcite and/or dolomite (though not at a sufficiently high content to be identified by XRD analysis), and the Mg and Al being hosted by clinocllore. The dissolved Si also derives from clinocllore, but it is apparent that fractions remain in undissolved solids and/or precipitate from the solution to generate amorphous silica. Talc present in the concentrate is expected to be refractory, and this is consistent with the mineralogical characterization data [35].

5.5. Additives Other Than Chloride Salts

5.5.1. Effect of Sodium Sulphate Addition

The comparison of no salt versus salt additions and the effect upon copper extraction under pressure oxidation conditions has been discussed in Sections 5.1.1 and 5.1.2. As noted there, the addition of NaCl (2.8 M) enables chalcopyrite extraction, whereby near-quantitative copper leaching occurs on a shorter timescale. It was also notable that addition of Na_2SO_4 (1.4 M) enhanced the initial rate of extraction, although it is expected that the solubility of oxygen in this process liquor will be smaller than that for no additive, based on the model developed by Tromans [114,115]. While it was noted in Section 5.1.2 that upfront addition of sulphuric acid slows chalcopyrite extraction, the addition of Na_2SO_4 buffers the sulphuric acid generated [136], over and above that due to copper sulphate formation, thereby slightly enhancing chalcopyrite extraction when compared to no salt addition. This is also reflected in the data shown, which indicate that free acid formation was marginally greater when Na_2SO_4 was added (~99 g/L), though this can also be explained by concentrate sub-sample variation, i.e., use of a sub-sample with a marginally higher

sulphide content. Whereas the lower free acidity in other tests for which the pulp density is the same is accompanied by the formation of basic iron sulphate phases in the leach residue, hematite formation was promoted by Na_2SO_4 addition. This topic is discussed further elsewhere [35].

5.5.2. Effects of Aluminium Addition

Upfront addition of aluminium-containing materials to the chalcopyrite concentrate was investigated as a means of influencing the chemistry of the system, and more particularly, the leach residue mineralogy [35]. Two aluminium sources were used in the current tests to double the aluminium content: aluminium sulphate, $\text{Al}_2(\text{SO}_4)_3 \cdot 18\text{H}_2\text{O}$, and gibbsite, $\text{Al}(\text{OH})_3$. The impacts upon copper extraction kinetics and the free acidity of the leach liquor were small (Figure 14). In relation to free acidity, aluminium sulphate addition was expected to generate acid due to aluminium hydrolysis to form (natro)alunite, while the addition of gibbsite would result in a net loss of acid even though the dissolved aluminium hydrolyses form (natro)alunite: the net reactions are indicated by Equations (10) and (11). A small decrease in the free acid level was indeed noted when gibbsite was added. In contrast, aluminium sulphate addition did not notably increase the free acidity, and this can be explained by a fraction of the iron reporting to the (natro)alunite phase rather than hematite [35].

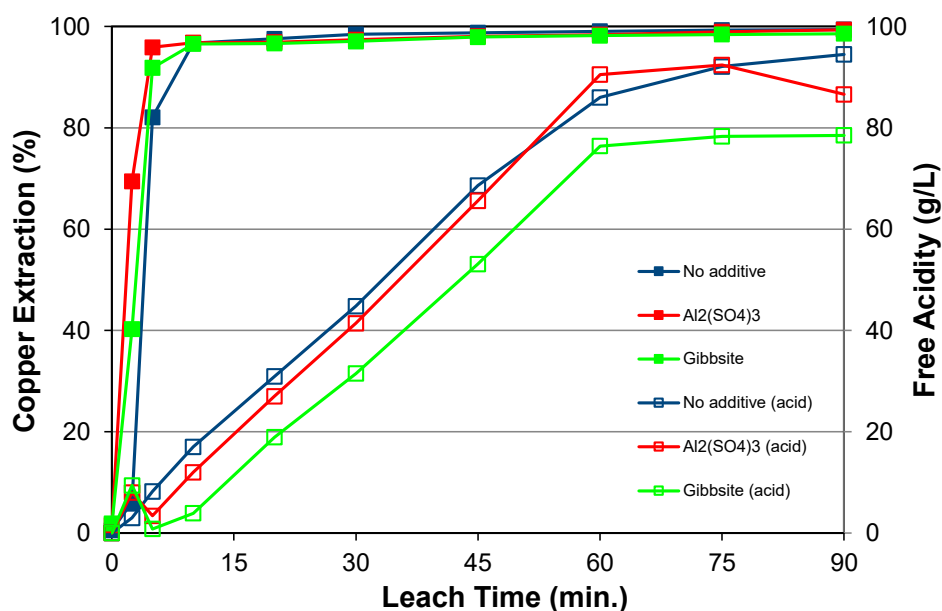
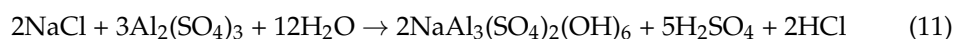
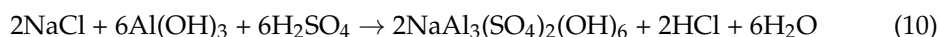


Figure 14. Effect of aluminium-containing additives on the leaching of chalcopyrite concentrate ($P_{100} - 45 \mu\text{m}$) under pressure oxidation conditions ($220 \text{ }^\circ\text{C}$, 700 kPa O_2 , $20\% w/w$ pulp density, 15 g/L Cl added as NaCl). Additions of aluminium sulphate and gibbsite were performed to double the aluminium content of the system.

5.6. Reaction Kinetics

The leach kinetics for chalcopyrite have been demonstrated to follow a shrinking-core model for various media (e.g., sulphate, chloride, and nitrate) and various oxidants, including ferric iron, oxygen, and hydrogen peroxide, though the specific form of the model is either surface- or diffusion-controlled, depending on the experimental parameters used, which have been noted to vary between different studies [23]. For example, at low temperatures (60–90 °C) and in sulphate medium, chalcopyrite leaching is best represented by a model involving transport through a reaction product layer [137]. The study of Li et al. [138] at temperatures between 35 and 75 °C, however, suggests that the reaction was chemically controlled during the early stages, and then surface diffusion-controlled later. Others (e.g., [20]) have arrived at a similar conclusion for low-temperature chalcopyrite leaching. Notably, Yue and Asselin [139] concluded that control of chalcopyrite leaching in the sulphate system at temperatures up to 150 °C depends on the solution composition and temperature.

Hidalgo et al. [140] surveyed leaching mechanisms for ferric iron in both sulphate and chloride systems, concluding that in chloride, chalcopyrite leaching at temperatures up to 100 °C is surface reaction-controlled. In contrast, the data of Baba et al. [141] for the leaching of chalcopyrite in hydrochloric acid suggested the reaction was diffusion-controlled, noting that other studies in chloride media indicated both chemical- and diffusion-controlled kinetics.

While Baba et al. [142] suggested that chalcopyrite leaching in nitric acid was diffusion-controlled for temperatures in the range 27–80 °C, Sokić et al. [143] determined that a mixed-control model best-described such leaching by sodium nitrate in sulphuric acid in the range 70–90 °C. The form of the model used, which is a simplified version of the Avrami–Erofeev or KEKAM (Kolmogorov–Erofeev–Kazeev–Avrami–Mampel) equation for $n = 1$, is given by the following expression:

$$K_r t = -\ln(1 - X) \quad (12)$$

where K_r is the reaction rate, X represents the extent of the reaction (normally determined from copper extraction), and t is the reaction time. This can be used to identify the regions where chemical and diffusion control are dominant, though it was noted that there appears to be a region of the plot where mixed control occurs. Such behaviour can also be modelled by the shrinking-core mixed-model, which can be written as:

$$K_r t = 1 - (1 - X)^{\frac{1}{3}} + B \left[1 - \frac{2}{3} X - (1 - X)^{\frac{2}{3}} \right] \quad (13)$$

where the value for B is estimated from fitting the chemical rate control equation to the initial kinetic data to determine the chemical rate constant [144].

In the present study, kinetic analysis of copper extraction for selected experiments was undertaken. The starting point was the general Avrami–Erofeev equation, which can be expressed in linear form as:

$$\ln[-\ln(1 - X)] = n \ln t + \ln K_r \quad (14)$$

Plots of data using this equation for tests without added chloride are shown in Figure 15. For upfront acid additions of 0 g/L (pulp density 10% or 20% w/w) and 30 g/L (pulp density 20% w/w), the slopes (fitted to data for which the last point corresponded to the first sample, having copper extraction of above 90%) within experimental error correspond to a value of 1, suggesting that the reaction is chemically controlled; even for an acid addition of 100 g/L (pulp density 20% w/w), the slope was only marginally larger.

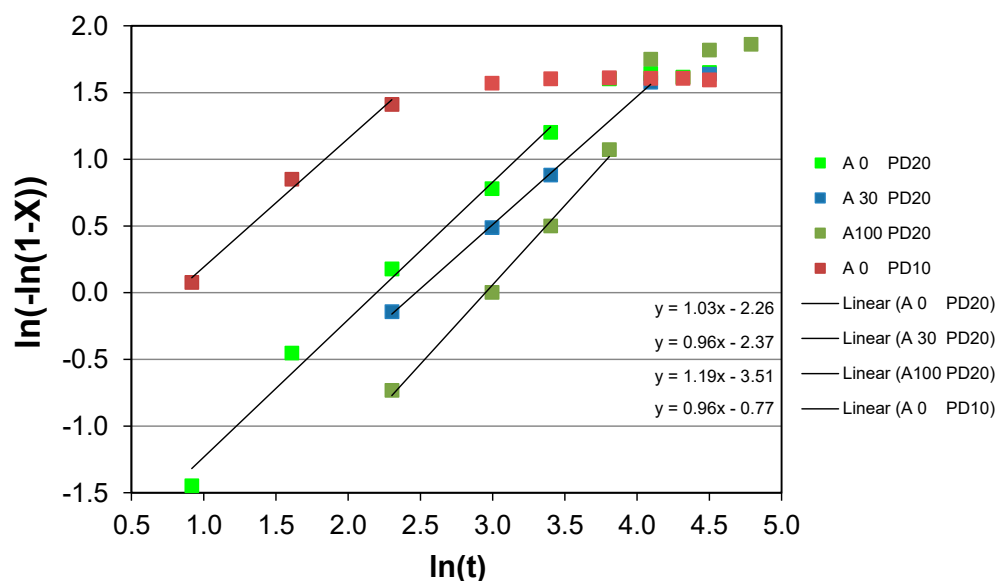


Figure 15. Plots of the linear form of the Avrami–Erofeev equation for the leaching of chalcopyrite concentrate ($P_{100} - 45 \mu\text{m}$) under pressure oxidation conditions ($220 \text{ }^\circ\text{C}$, 700 kPa O_2) with varying pulp densities (% w/w), no added chloride, and varying upfront acid addition (g/L). The best-fit equations are shown within the plot area for each set of data.

Copper extraction was substantially quicker during experiments where chloride was added, and therefore, Avrami–Erofeev plots generally only yielded two points for which a best-fit line could be obtained. This is neither considered to be acceptable for the validation of the reaction control mechanism nor the estimation of the corresponding reaction rate. The notable exception was when leaching was slowed using a lower-oxygen partial pressure, 100 kPa ($20\% w/w$ pulp density, 15 g/L chloride). Although not shown here, the slope derived from three points was significantly greater, at 4.6 . As the slope increased above 1 , the kinetics of the reaction began to impact the reaction control mechanism, and this has been noted in other studies where the value of n has been found to vary [145]. It is notable for each plot that data points obtained later during the reaction fit poorly to Equation (14). This is hypothesised to be due to encapsulation of the chalcopyrite by pyrite (while a trace amount might also be hosted within silicate minerals), which reacts more slowly, hindering the extraction of the final fraction of the copper until much later during the experiments. It is also possible that copper forms metathesis product(s) at exposed pyrite surfaces [93,146], which will remain a sink for copper until all the pyrite has reacted. Furthermore, any loss of copper from solution to residue phases, such as hematite, will also affect the copper extraction achieved.

The values of the intercepts shown in Figure 15 correspond to reaction rate (K_r) values of 0.104 , 0.093 , and 0.030 , respectively, for acid additions of 0 , 30 , and 100 g/L , respectively. This is consistent with the impact of increasing the acid addition upon slowing chalcopyrite leaching, as shown in Figure 4. By decreasing the pulp density from $20\% w/w$ to $10\% w/w$ (with no addition), the K_r value increased to 0.463 , and this is consistent with the rate of copper extraction increasing with the decreasing pulp density (Figure 2).

Others have also examined chalcopyrite leaching kinetics using a similar approach to that applied here. Returning to the study of Sokić et al. [143], at lower temperatures, $70\text{--}75 \text{ }^\circ\text{C}$, and extents of copper extraction, i.e., $<60\%$, chalcopyrite leaching was suggested to be chemically controlled, whereas at higher temperatures, $80\text{--}90 \text{ }^\circ\text{C}$, and at higher copper extraction, i.e., $>60\%$, control by diffusion through an elemental sulphur layer was identified. The calculated values for n in Equation (14) varied between 0.6 and 0.8 under chemical control and between 0.2 and 0.5 under diffusion control. The calculated activation energy (83 kJ/mol) from modelling of the extraction regions proposed under chemical control used this proposition. The study by Petrović et al. [147] of chalcopyrite leaching with hydrogen

peroxide in hydrochloric acid over the temperature range 30–60 °C employed a version of the KEKAM model (modified to adjust for the maximum copper extraction). In this instance, the reaction was indicated to be controlled by diffusion through a product layer, with a calculated activation energy of 19.6 kJ/mol. For systems containing metals where chemical control is expected, e.g., scheelite in hydrochloric acid, the slope of the Avrami–Erofeev plot was confirmed to be 1 [148]. From this study, variation in the calculated values for n in Equation (14) between 0.97 and 1.17 was noted, not unlike the variation indicated in Figure 15.

To provide validation for the approach previously described, kinetic analysis was conducted using data from the slowest reaction studied: 220 °C, 20% pulp density, 100 g/L of acid, and no chloride additions. Several shrinking-core models applied to chalcopyrite leaching, as described in the review of Li et al. [23], were applied, as given by Equations (15)–(17):

$$\text{Chemical control : } K_r t = 1 - (1 - X)^{\frac{1}{3}} \quad (15)$$

$$\text{Diffusion through product layer 1 : } K_r t = 1 + 2(1 - X) - 3(1 - X)^{\frac{2}{3}} \quad (16)$$

$$\text{Diffusion through product layer 2 : } K_r t = (1 - (1 - X)^{\frac{1}{3}})^2 \quad (17)$$

The model plots presented in Figure 16 clearly indicate that for the slowest reaction, it is best described by a chemical control mechanism. This is consistent with the conclusion obtained from the analysis using the Avrami–Erofeev equation. The interpretation of modelling data for other reactions may be less clear-cut, and this is shown in Figure 17. Here, the regression fits were determined for copper extractions up to 96.4% for a reaction indicated from K_r values to be around 3.5 times faster: 220 °C, 20% pulp density, and no acid or chloride additions. The regression coefficients for models described by Equations (15)–(17) were 0.959, 0.991, and 0.976, suggesting that the leaching mechanism is best described by diffusion through a product layer, though none of the straight-line fits could be considered poor. The suggestion of a product layer diffusion-controlled mechanism, however, seems inconsistent with the mineralogical data for this experiment, as only trace amounts of covellite intermediate and elemental sulphur were detected in the leach residues [35].

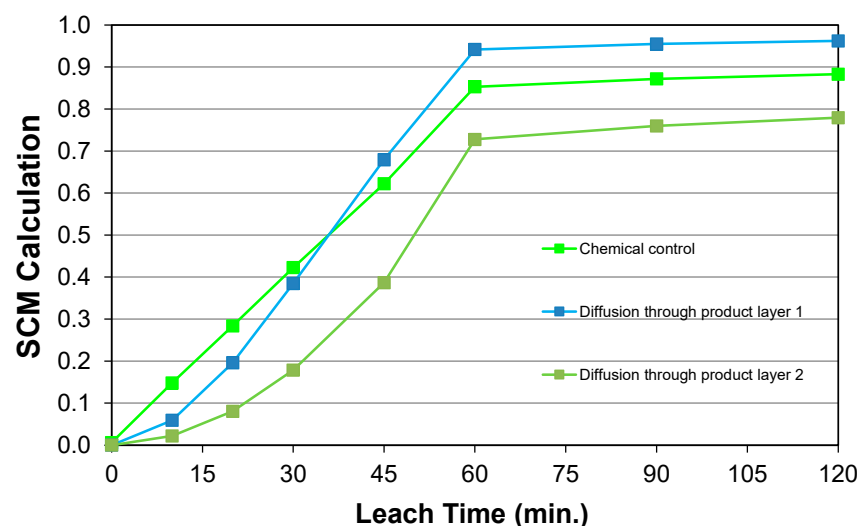


Figure 16. Modelling of the reaction kinetics using selected shrinking-core models for the leaching of chalcopyrite concentrate ($P_{100} - 45 \mu\text{m}$) under pressure oxidation conditions (220 °C, 20% w/w pulp density, 700 kPa O_2), no added chloride, and a 100 g/L upfront acid addition. The equations for the shrinking-core models (SCMs) used to obtain the Y-axis data are presented in the text.

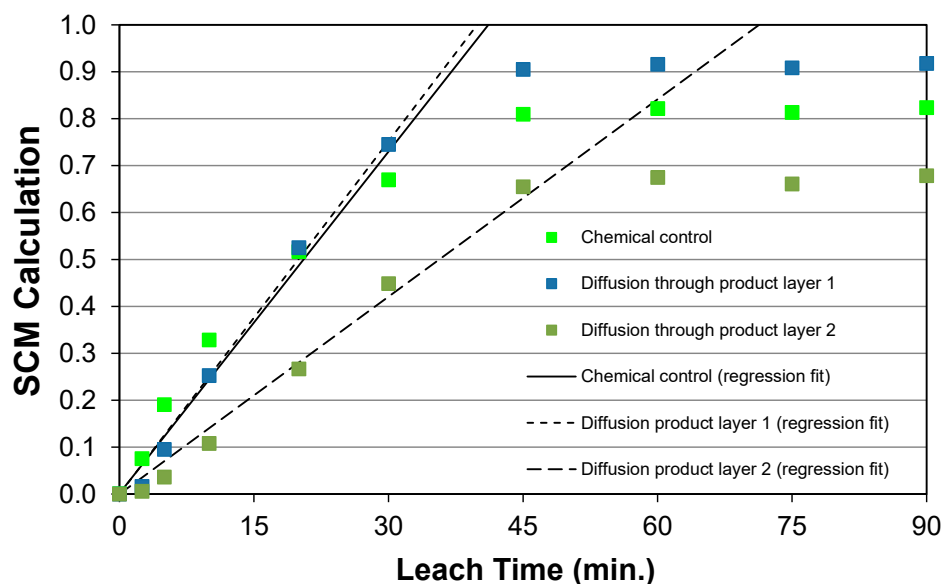


Figure 17. Modelling of the reaction kinetics using selected shrinking-core models for the leaching of chalcopyrite concentrate ($P_{100} - 45 \mu\text{m}$) under pressure oxidation conditions ($220 \text{ }^\circ\text{C}$, $20\% w/w$ pulp density, 700 kPa O_2), no added chloride, and no upfront acid addition. The equations for the shrinking-core models (SCMs) used to obtain the Y-axis data are presented in the text.

Prosser [149] undertook a review of the uncertainties that might impact the interpretation of reaction mechanisms. Of specific relevance to this study are topics examining the determination of the extent of the reaction (and errors associated with this measurement) and the selection and application of model equations to determine if these are consistent with the data. Critical to the selection of a specific model are the assumptions that are built into that model. It is also noted that the modelling of the reaction extent is normally based on the concentration of the dissolved product, and rarely is the measurement of unreacted minerals during the reaction performed. This last point brings the discussion back to the impact of chloride on enhancing the leaching rate of chalcopyrite. As previously noted, the small number of data points generated in this study during the period when most of the leaching occurred, i.e., 5–10 min, are insufficient to identify a kinetic model that best describes the reaction. Consequently, the calculation of the activation energy for the reaction was not possible. To improve the kinetic analysis of reactions examined in this study, higher-resolution sample data, including both elemental extraction and quantitative mineralogical data, need to be obtained. This would also require reactions to be conducted using conditions that are not commercial, whereby the rate of oxidation is sufficiently slowed, i.e., using oxygen overpressure $\ll 100 \text{ kPa}$, or by controlling the mass rate at which oxygen is injected into the system, e.g., via a mass flow controller. Finally, it is recognised that both the chalcopyrite and covellite phases contribute to the overall reaction mechanism; therefore, kinetic analysis should aim to deconvolute the contributions from the chalcopyrite to covellite conversion and the dissolution of the covellite to enable these reaction rates as a function of temperature, and hence meaningful estimates for their activation energies to be obtained.

6. Conclusions

High-temperature ($\geq 220 \text{ }^\circ\text{C}$) pressure oxidation of a chalcopyrite concentrate was studied in batch mode for most experiments using a 700 kPa O_2 partial pressure under various conditions. Pulp densities of either 10% or $20\% w/w$ were employed, and the impacts of dissolved chloride, sulphuric acid addition, and other selected additives on copper extraction kinetics and oxidation mechanisms were examined over times normally up to 90 min .

Chloride addition enhanced the rate of copper extraction, whereas the added sulphuric acid slowed dissolution. The addition of chloride favours an oxidation mechanism that rapidly transforms chalcopyrite into a covellite intermediate, that when dissolved liberates cupric ions and forms elemental sulphur. The reactions of the copper sulphide phases were hypothesised to involve a surface chloride-mediated rate-determining step, also noting that the reaction of covellite was typically faster than chalcopyrite. That the elemental sulphur formed reacted subsequent to, and more slowly than, the leaching of the covellite intermediate provides clear evidence for the decoupling of the copper oxidation/extraction and sulphate formation reactions. Elemental sulphur was slowly oxidised, typically resulting in a linear increase in free acidity/dissolved sulphur species at times of up to 60 min in tests employing a 20% *w/w* pulp density. In contrast, most of the copper was typically extracted within 5–10 min.

The impact of decreasing the oxygen partial pressure from 700 to 100 kPa was small compared to that reported for previous studies at lower temperatures, and this was estimated to decrease the reaction rate by just over half. Increasing the reaction temperature from 220 to 230 °C, and ultimately 245 °C, resulted in more rapid generation of sulphuric acid and decreased the iron concentration in the leach liquor.

Analysis of kinetic data using an Avrami–Erofeev model clearly indicated that copper dissolution was chemically controlled under the conditions employed. The slowing of the reaction as copper extraction approached unity was proposed to indicate that a small fraction of the chalcopyrite may be physically encapsulated by pyrite (which is the last sulphide mineral to be dissolved), and/or by refractory silicate minerals, e.g., quartz. It is also possible that some copper was hydrothermally incorporated into the (accessible) pyrite structure during the reaction, and therefore, only released once pyrite was completely dissolved.

The kinetic data analysis undertaken here was not comprehensive as the leaching of chalcopyrite in the presence of chloride was often complete within 5–10 min. This meant that the resolution of sample data was often insufficient to enable meaningful kinetic analysis, and from this, the estimation of activation energies to be undertaken. It is recommended that further work on this topic is undertaken using process conditions for which the rate of oxidation is significantly decreased.

Funding: The funding for some of the work reported here was provided by the Parker Centre for Integrated Hydrometallurgical Solutions.

Data Availability Statement: The data are not publicly available due to privacy issues.

Acknowledgments: This study is dedicated to the memory of David M. Muir as an acknowledgement of his significant achievements in the field of hydrometallurgy and his mentorship of the author during his time at CSIRO. The author also wishes to thank staff from the Analytical and Materials Characterisation group at CSIRO Mineral Resources, Waterford, both past and present, for their assistance in providing the analytical and XRD measurements.

Conflicts of Interest: The author declares no conflict of interest.

References

1. Kruesi, P.R.; Allen, E.S.; Lake, J.L. Cymet Process—Hydrometallurgical conversion of base- metal sulphides to pure metals. *CIM Bulletin* **1973**, *66*, 81–87.
2. Dalton, R.F.; Diaz, G.; Price, R.; Zunkel, A.D. The Cuprex metal extraction process: Recovering copper from sulfide ores. *JOM* **1991**, *43*, 51–56. [[CrossRef](#)]
3. Moyes, J.; Sammut, D.; Houllis, F. The Intec Copper Process: Superior and Sustainable Metals Production. In Proceedings of the ALTA 2002 Copper 7 Conference, Perth, Australia, 23–24 May 2002; ALTA Metallurgical Services: Melbourne, Australia, 2002. 22p.
4. Hourn, M.M.; Turner, D.W.; Holzberger, I.R. Atmospheric mineral leaching process. U.S. Patent 5,993,635A1, 30 November 1999.
5. Lundström, M.; Aromaa, J.; Forsén, O.; Hyvärinen, O.; Barker, M.H. Leaching of chalcopyrite in cupric chloride solution. *Hydrometallurgy* **2005**, *77*, 89–95. [[CrossRef](#)]
6. Nazari, G.; Dixon, D.G.; Dreisinger, D. Enhancing the kinetic of chalcopyrite leaching in the GalvanoxTM process. *Hydrometallurgy* **2011**, *105*, 251–258. [[CrossRef](#)]

7. Chaiko, D.; Baczek, F.; Rocks, S.S.; Walters, T.; Klepper, R. The FLSmidth® rapid-oxidative leach (ROL) process Part I: Mechanochemical process for treating chalcopyrite. Proceeding of the COM2015, Conference of Metallurgists, Montreal, QC, Canada; Canadian Institute of Mining, Metallurgy and Petroleum: Montreal, QC, Canada, 2015. 11p.
8. Chaiko, D.; Rocks, S.S.; Walters, T.; Asihene, S.; Eyzaguirre, C.; Klepper, R.; Baczek, F.; McMahon, G. The FLSmidth® rapid-oxidative leach (ROL) process Part II: A new chemical activation process for chalcopyrite. In *COM2015, Conference of Metallurgists*; Canadian Institute of Mining, Metallurgy and Petroleum: Montreal, QC, Canada, 2015; 15p.
9. Mulligan, M.; Chaiko, D.; Baczek, F.; Rocks, S.; Eyzaguirre, C.; Dickinson, C.; Klepper, R. The FLSmidth® Rapid Oxidative Leach (ROL) process: A mechano-chemical approach and industrial applications for rapid metal sulphide dissolution. *J. South. Afr. Inst. Min. Metall.* **2017**, *117*, 741–747. [[CrossRef](#)]
10. Oraby, E.A.; Eksteen, J.J. The selective leaching of copper from a gold–copper concentrate in glycine solutions. *Hydrometallurgy* **2014**, *150*, 14–19. [[CrossRef](#)]
11. Evans, H.A.; Johnson, G.D. Activox® Technology for treatment of copper sulfide concentrates. In Proceedings of the International Conference of Randol, Copper Hydromet Roundtable '99, Phoenix, AZ, USA, 10–13 October 1999; Randol International: Golden, CO, USA, 1999. 3p.
12. Subramanian, K.N.; Jennings, P.H. Review of the hydrometallurgy of chalcopyrite concentrates. *Can. Metall. Q.* **1972**, *11*, 387–400. [[CrossRef](#)]
13. Dutrizac, J.E. The leaching of sulphide minerals in chloride media. *Hydrometallurgy* **1992**, *27*, 1–45. [[CrossRef](#)]
14. Venkatachalam, S. Treatment of chalcopyrite concentrates by hydrometallurgical techniques. *Miner. Eng.* **1991**, *4*, 1115–1126. [[CrossRef](#)]
15. Prasad, S.; Pandey, B.D. Alternative processes for treatment of chalcopyrite. *Miner. Eng.* **1998**, *11*, 763–781. [[CrossRef](#)]
16. Berezowsky, R.; Trytten, L. Commercialization of the acid pressure leaching of chalcopyrite. In Proceedings of the ALTA 2002 Copper 7 Conference, Perth, Australia, 23–24 May 2002; ALTA Metallurgical Services: Melbourne, Australia, 2002. 40p.
17. Dreisinger, D. Copper leaching from primary sulfides: Options for biological and chemical extraction of copper. *Hydrometallurgy* **2006**, *83*, 10–20. [[CrossRef](#)]
18. Dreisinger, D.B. Case study flowsheets: Copper–gold concentrate treatment. In *Gold Ore Processing*, 2nd ed.; Adams, M.D., Ed.; Elsevier B.V.: Amsterdam, The Netherlands, 2016; pp. 803–820.
19. Baba, A.A.; Ayinla, K.I.; Adekola, F.A.; Ghosh, M.K.; Ayanda, O.S.; Bale, R.B.; Sheik, A.R.; Pradhan, S.R. A review on novel techniques for chalcopyrite ore processing. *Int. J. Min. Eng. Miner. Process.* **2012**, *1*, 1–16. [[CrossRef](#)]
20. Klauber, C. A critical review of the surface chemistry of acidic ferric sulphate dissolution of chalcopyrite with regards to hindered dissolution. *Int. J. Miner. Process.* **2008**, *86*, 1–17. [[CrossRef](#)]
21. Córdoba, E.M.; Muñoz, J.A.; Blázquez, M.L.; González, F.; Ballester, A. Leaching of chalcopyrite with ferric ion. Part I: General aspects. *Hydrometallurgy* **2008**, *93*, 81–87. [[CrossRef](#)]
22. Córdoba, E.M.; Muñoz, J.A.; Blázquez, M.L.; González, F.; Ballester, A. Leaching of chalcopyrite with ferric ion. Part II: Effect of redox potential. *Hydrometallurgy* **2008**, *93*, 88–96. [[CrossRef](#)]
23. Li, Y.; Kawashima, N.; Li, J.; Chandra, A.P.; Gerson, A.R. A review of the structure, and fundamental mechanisms and kinetics of the leaching of chalcopyrite. *Adv. Colloid Interface Sci.* **2013**, *197*, 1–32. [[CrossRef](#)]
24. Watling, H.R. Chalcopyrite hydrometallurgy at atmospheric pressure: 1. Review of acidic sulfate, sulfate–chloride and sulfate–nitrate process options. *Hydrometallurgy* **2013**, *140*, 163–180. [[CrossRef](#)]
25. Watling, H.R. Chalcopyrite hydrometallurgy at atmospheric pressure: 2. Review of acidic chloride process options. *Hydrometallurgy* **2014**, *146*, 96–110. [[CrossRef](#)]
26. Barton, I.F.; Hiskey, J.B. Chalcopyrite leaching in novel lixiviants. *Hydrometallurgy* **2022**, *207*, 105775. [[CrossRef](#)]
27. Marsden, J.O.; Brewer, R.E.; Hazen, N. Copper concentrate leaching developments by Phelps Dodge Corporation. In Proceedings of the Hydrometallurgy 2003—Fifth International Conference in Honour of Professor Ian Ritchie, Volume 2: Electrometallurgy and Environmental Hydrometallurgy, Vancouver, BC, Canada, 24–27 August 2003; Young, C.A., Alfantazi, A.M., Anderson, C.G., Dreisinger, D.B., Harris, B., James, A., Eds.; TMS: Warrendale, PA, USA; pp. 1429–1446.
28. Marsden, J.O.; Wilmot, J.C.; Mathern, D.R. Medium-temperature pressure leaching of copper concentrates—Part III. Commercial demonstration plant at Bagdad Arizona. *Miner. Metall. Process.* **2007**, *24*, 218–225.
29. Green, C.; Robertson, J.; Marsden, J.O. Pressure leaching of copper concentrates at Morenci, Arizona—10 years of experience. *Miner. Metall. Process.* **2018**, *35*, 109–116. [[CrossRef](#)]
30. Voigt, P.; Stieper, G.; Hourn, M. First commercialization of the Albion Process™ for copper. In Proceedings of the 58th Annual Conference of Metallurgists Hosting the 10th International Copper Conference 2019, COM 2019, Vancouver, BC, Canada, 18–21 August 2019; MetSoc: Montreal, QC, Canada, 2019. 13p.
31. Jones, D.L.; Mayhew, K.; O'Connor, L. Nickel and cobalt recovery from a bulk copper-nickel concentrate using the CESL process. In *Hydrometallurgy of Nickel and Cobalt, Proceedings of the 48th Annual Conference of Metallurgists of CIM, Sudbury, ON, Canada, 23–26 August 2009*; Budac, J.J., Fraser, R., Mihaylov, I., Papangelakis, V.G., Robinson, D.J., Eds.; MetSoc: Montreal, QC, Canada, 2009; pp. 45–57.
32. Wardell-Johnson, M.; Steiper, G.; Dreisinger, D. Engineering aspects of the Platsol™ process. In Proceedings of the ALTA 2009 Nickel/Cobalt 14 Conference, Perth, Australia, 25–27 May 2009; ALTA Metallurgical Services: Melbourne, Australia, 2009. 20p.
33. Dreisinger, D.; Molnar, R.; Mezei, A.; Baxter, K.; Wardell-Johnson, M. The recovery of nickel and cobalt from the NorthMet deposit using the Platsol™ process with production of mixed or separate nickel and cobalt hydroxides. In *Hydrometallurgy of Nickel*

- and Cobalt, *Proceedings of the 48th Annual Conference of Metallurgists of CIM, Sudbury, ON, Canada, 23–26 August 2009*; Budac, J.J., Fraser, R., Mihaylov, I., Papangelakis, V.G., Robinson, D.J., Eds.; MetSoc: Montreal, QC, Canada, 2009; pp. 123–138.
34. Karcz, A.P.; Damø, A.J.; Illerup, J.B.; Rocks, S.; Dam-Johansen, K.; Chaiko, D. Electron microscope investigations of activated chalcopyrite particles via the FLSmith[®] ROL process. *J. Mater. Sci.* **2017**, *52*, 12044–12053. [[CrossRef](#)]
 35. McDonald, R.G. The effects of chloride on the high temperature pressure oxidation of chalcopyrite: Some insights from batch tests—Part 2. Leach residue mineralogy. *Miner. Eng.* **2023**, *in press*.
 36. Weidenbach, M.; Dunn, G.; Teo, Y.Y. Removal of impurities from copper sulphide mineral concentrates. In *Proceedings of the ALTA 2016 Copper 7 Forum, Perth, Australia, 21–28 May 2016*; ALTA Metallurgical Services: Melbourne, Australia, 2016; pp. 335–351.
 37. Fomenko, I.V.; Pleshkov, M.A.; Shneerson, Y.M.; Ospanov, E.A.; Shakhlov, A.A.; Naboychenko, S.S. Low-grade copper concentrate purification and enrichment by complex pressure oxidation—Hydrothermal alteration technology. In *Proceedings of the 58th Annual Conference of Metallurgists Hosting the 10th International Copper Conference 2019, COM 2019, Vancouver, BC, Canada, 18–21 August 2019*; MetSoc: Montreal, QC, Canada, 2019. 13p.
 38. Chaudhari, A.; Webster, N.A.; Xia, F.; Friedrich, A.; Ram, R.; Etschmann, B.; Liu, W.; Wykes, J.; Brand, H.E.; Brugger, J. Anatomy of a complex mineral replacement reaction: Role of aqueous redox, mineral nucleation, and ion transport properties revealed by an in-situ study of the replacement of chalcopyrite by copper sulfides. *Chem. Geol.* **2021**, *581*, 120390. [[CrossRef](#)]
 39. McDonald, R.G.; Muir, D.M. Pressure oxidation leaching of chalcopyrite. Part I. Comparison of high and low temperature reaction kinetics and products. *Hydrometallurgy* **2007**, *86*, 191–205. [[CrossRef](#)]
 40. McDonald, R.G.; Muir, D.M. Pressure oxidation leaching of chalcopyrite. Part II. Comparison of medium temperature kinetics and products and effect of chloride ion. *Hydrometallurgy* **2007**, *86*, 206–220. [[CrossRef](#)]
 41. Hackl, R.P.; Dreisinger, D.B.; Peters, E.; King, J.A. Passivation of chalcopyrite during oxidative leaching in sulphate media. *Hydrometallurgy* **1995**, *39*, 25–48. [[CrossRef](#)]
 42. Petersen, A.E. Oxidation leaching. CA Patent 1263540A, 12 May 1989.
 43. Viramontes-Gamboa, G.; Rivera-Vasquez, B.F.; Dixon, D.G. The active-passive behaviour of chalcopyrite: Comparative study between electrochemical and leaching responses. *J. Electrochem. Soc.* **2007**, *154*, C299–C304. [[CrossRef](#)]
 44. Lundström, M.; Aromaa, J.; Forsén, O. The rate-controlling step of chalcopyrite dissolution in concentrated cupric chloride solution. In *Copper 2010*; Harre, J., Ed.; GDMB: Clausthal-Zellerfeld, Germany, 2010; Volume 5, pp. 1959–1972.
 45. Velásquez-Yévenes, L.; Nicol, M.; Miki, H. The dissolution of chalcopyrite in chloride solutions. Part 1. The effect of solution potential. *Hydrometallurgy* **2010**, *103*, 113–118. [[CrossRef](#)]
 46. Nicol, M.; Miki, H.; Zhang, S. The anodic behaviour of chalcopyrite in chloride solutions: Voltammetry. *Hydrometallurgy* **2017**, *171*, 198–205. [[CrossRef](#)]
 47. Debernardi, G.; Gentina, J.C.; Albistur, P.; Slanzi, G. Evaluation of processing options to avoid the passivation of chalcopyrite. *Int. J. Miner. Process.* **2013**, *125*, 1–4. [[CrossRef](#)]
 48. Yin, Q.; Kelsall, G.H.; Vaughan, D.J.; England, K.E.R. Atmospheric and electrochemical oxidation of the surface of chalcopyrite (CuFeS₂). *Geochim. Cosmochim. Acta* **1995**, *59*, 1091–1100. [[CrossRef](#)]
 49. Liu, Q.; Chen, M.; Yang, Y. The effect of chloride ions on the electrochemical dissolution of chalcopyrite in sulfuric acid solutions. *Electrochim. Acta* **2017**, *253*, 257–267. [[CrossRef](#)]
 50. Ren, Z.; Chao, C.; Krishnamoorthy, P.; Asselin, E.; Dixon, D.G.; Mora, N. The overlooked mechanism of chalcopyrite passivation. *Acta Mater.* **2022**, *236*, 118111. [[CrossRef](#)]
 51. Winand, R. Chloride hydrometallurgy. *Hydrometallurgy* **1991**, *27*, 285–316. [[CrossRef](#)]
 52. Wang, S. Copper leaching from chalcopyrite concentrates. *JOM* **2005**, *57*, 48–51. [[CrossRef](#)]
 53. Lundström, M.; Aromaa, J.; Forsén, O.; Haavanlammi, L. Concentrated cupric chloride solutions: Possibilities offered in copper production. *Acta Metall. Slov.* **2007**, *13*, 447–459.
 54. Senanayake, G. A review of chloride assisted copper sulphide leaching by oxygenated sulphuric acid and mechanistic considerations. *Hydrometallurgy* **2009**, *98*, 21–32. [[CrossRef](#)]
 55. Torres, D.; Ayala, L.; Jeldres, R.I.; Cerecedo-Sáenz, E.; Salinas-Rodríguez, E.; Robles, P.; Toro, N. Leaching chalcopyrite with high MnO₂ and chloride concentrations. *Metals* **2020**, *10*, 107. [[CrossRef](#)]
 56. Kowalczyk, P.B.; Manaig, D.O.; Drivenes, K.; Snook, B.; Aasly, K.; Kleiv, R.A. Galvanic leaching of seafloor massive sulphides using MnO₂ in H₂SO₄-NaCl media. *Minerals* **2018**, *8*, 235. [[CrossRef](#)]
 57. Muñoz-Ribadeneira, F.J.; Gomberg, H.J. Leaching of chalcopyrite (CuFeS₂) with sodium chloride sulfuric acid solutions. *Nucl. Technol.* **1971**, *11*, 367–371. [[CrossRef](#)]
 58. Subramanian, K.N.; Ferrajuolo, R. Oxygen pressure leaching of Fe-Ni-Cu sulphide concentrates at 110 °C—Effect of chloride addition. *Hydrometallurgy* **1976**, *2*, 117–125. [[CrossRef](#)]
 59. Sullivan, J.D. Chemical and physical features of copper leaching. *Trans. Am. Inst. Min. Metall. Eng.* **1933**, *106*, 515–546.
 60. Habashi, F.; Toor, T. Aqueous oxidation of chalcopyrite by hydrochloric acid. *Metall. Trans. B Process Metall.* **1979**, *10B*, 49–56. [[CrossRef](#)]
 61. Dutrizac, J.E. The dissolution of chalcopyrite in ferric sulphate and ferric chloride media. *Metall. Trans. B Process Metall.* **1981**, *12B*, 49–56.
 62. Majima, H.; Awakura, Y.; Hirato, T.; Tanaka, T. The leaching of chalcopyrite in ferric chloride and ferric sulfate solutions. *Can. Metall. Q.* **1985**, *24*, 283–291. [[CrossRef](#)]

63. Hirato, T.; Kinoshita, M.; Awakura, Y.; Majima, H. The leaching of chalcopyrite with ferric chloride. *Metall. Trans. B Process Metall.* **1986**, *17B*, 19–28. [[CrossRef](#)]
64. Lu, Z.Y.; Jeffrey, M.I.; Lawson, F. The effect of chloride ions on the dissolution of chalcopyrite in acidic solutions. *Hydrometallurgy* **2000**, *56*, 189–202. [[CrossRef](#)]
65. Lu, Z.Y.; Jeffrey, M.I.; Lawson, F. An electrochemical study of the effect of chloride ion on the dissolution of chalcopyrite in acid solutions. *Hydrometallurgy* **2000**, *56*, 145–155. [[CrossRef](#)]
66. Skrobjan, M.; Havlik, T.; Ukasik, M. Effect of NaCl concentration and particle size on chalcopyrite leaching in cupric chloride solution. *Hydrometallurgy* **2005**, *77*, 109–114. [[CrossRef](#)]
67. Palmer, B.R.; Nebo, C.O.; Rau, M.F.; Fursteneau, M.C. Rate phenomena involved in the dissolution of chalcopyrite in chloride-bearing lixivants. *Metall. Trans. B Process Metall.* **1981**, *12*, 595–601. [[CrossRef](#)]
68. Carneiro, M.F.C.; Leão, V.A. The role of sodium chloride on surface properties of chalcopyrite leached with ferric sulphate. *Hydrometallurgy* **2007**, *87*, 73–82. [[CrossRef](#)]
69. Yoo, K.; Kim, S.; Lee, J.; Ito, M.; Tsunekawa, M.; Hiroyoshi, M. Effect of chloride ions on the leaching rate of chalcopyrite. *Miner. Eng.* **2010**, *23*, 471–477. [[CrossRef](#)]
70. Whittington, B.I.; McDonald, R.G.; Johnson, J.A.; Muir, D.M. Pressure acid leaching of arid-region nickel laterite ore: Part I: Effect of water quality. *Hydrometallurgy* **2003**, *70*, 31–46. [[CrossRef](#)]
71. Bruce, R.; Seaman, T. Reducing Freshwater Use in the Production of Metals. Teck Resources Limited. 2014. Available online: <https://www.teck.com/media/CESL-Publication-Copper-reducing-fresh-water-use-in-the-production-of-metals.pdf> (accessed on 4 July 2022).
72. Toro, N.; Gálvez, E.; Robles, P.; Castillo, J.; Villca, G.; Salinas-Rodríguez, E. Use of alternative water resources in copper leaching processes in Chilean mining industry—A Review. *Metals* **2022**, *12*, 445. [[CrossRef](#)]
73. Padilla, R.; Rodríguez, G.; Ruiz, M.C. Copper and arsenic dissolution from chalcopyrite-enargite concentrate by sulfidation and pressure leaching in H₂SO₄-O₂. *Hydrometallurgy* **2010**, *100*, 152–156. [[CrossRef](#)]
74. Ruiz, M.C.; Montes, K.; Padilla, R. Pressure leaching of a chalcopyrite concentrate. In *Copper 2010*; Harre, J., Ed.; GDMB: Clausthal-Zellerfeld, Germany, 2010; Volume 5, pp. 2017–2027.
75. Peters, E. Direct leaching of sulfides: Chemistry and applications. *Metall. Trans. B Process Metall.* **1976**, *7*, 505–517. [[CrossRef](#)]
76. Peters, E. The electrochemistry of sulphide minerals. In *Trends in Electrochemistry*; Bockris, J.O.M., Rand, D.A.F., Welch, R.J., Eds.; Plenum Press: New York, NY, USA, 1977; pp. 267–290.
77. Huang, H.H. The Eh-pH diagram and its advances. *Metals* **2016**, *6*, 23. [[CrossRef](#)]
78. Hawker, W.; Byrne, K.; Vaughan, J. Upgrading copper sulphide concentrates through high temperature metathesis reactions. In Proceedings of the 58th Annual Conference of Metallurgists Hosting the 10th International Copper Conference 2019, COM 2019, Vancouver, BC, Canada, 18–21 August 2019; MetSoc: Montreal, QC, Canada, 2019. 10p.
79. Velásquez-Yévenes, L.; Miki, H.; Nicol, M. The dissolution of chalcopyrite in chloride solutions: Part 2: Effect of various parameters on the rate. *Hydrometallurgy* **2010**, *103*, 80–85. [[CrossRef](#)]
80. Jafari, M.; Karimi, G.; Ahmadi, R. Improvement of chalcopyrite atmospheric leaching using controlled slurry potential and additive treatments. *Physicochem. Probl. Miner. Process.* **2017**, *53*, 1228–1240.
81. Koleini, S.J.; Aghazadeh, V.; Sandström, Å. Acidic sulphate leaching of chalcopyrite concentrates in presence of pyrite. *Miner. Eng.* **2011**, *24*, 381–386. [[CrossRef](#)]
82. Hiroyoshi, N.; Kitagawa, H.; Tsunekawa, M. Effect of solution composition on the optimum redox potential for chalcopyrite leaching in sulphuric acid solutions. *Hydrometallurgy* **2008**, *91*, 144–149. [[CrossRef](#)]
83. Miki, H.; Nicol, M.; Velásquez-Yévenes, L. The kinetics of dissolution of synthetic covellite, chalcocite and digenite in dilute chloride solutions at ambient temperatures. *Hydrometallurgy* **2011**, *105*, 321–327. [[CrossRef](#)]
84. Cheng, C.Y.; Lawson, F. The kinetics of leaching covellite in acidic oxygenated sulphate-chloride solutions. *Hydrometallurgy* **1991**, *27*, 269–284. [[CrossRef](#)]
85. Kametani, H.; Aoki, A. Effect of suspension potential on the oxidation rate of copper concentrate in a sulfuric acid solution. *Metall. Trans. B Process Metall.* **1985**, *16*, 695–705. [[CrossRef](#)]
86. Harmer, S.L.; Thomas, J.E.; Fornasiero, D.; Gerson, A.R. The evolution of surface layers formed during chalcopyrite leaching. *Geochim. Cosmochim. Acta* **2006**, *70*, 4392–4402. [[CrossRef](#)]
87. Nava, D.; González, I. Electrochemical characterization of chemical species formed during the electrochemical treatment of chalcopyrite in sulphuric acid. *Electrochim. Acta* **2006**, *51*, 5295–5303. [[CrossRef](#)]
88. Ghahremaninezhad, A.; Asselin, E.; Dixon, D.G. Electrochemical evaluation of the surface of chalcopyrite during dissolution in sulfuric acid solution. *Electrochim. Acta* **2010**, *55*, 5041–5056. [[CrossRef](#)]
89. Ruiz, M.C.; Montes, K.S.; Padilla, R. Chalcopyrite leaching in sulfate-chloride media at ambient pressure. *Hydrometallurgy* **2011**, *109*, 37–42. [[CrossRef](#)]
90. Qiu, T.-S.; Nie, G.-H.; Wang, J.-F.; Ciu, L.-F. Kinetic process of oxidative leaching of chalcopyrite under low oxygen pressure and low temperature. *Trans. Nonferrous Metall. Soc. China* **2007**, *17*, 418–422. [[CrossRef](#)]
91. Hirato, T.; Majima, H.; Awakura, Y. The leaching of chalcopyrite with cupric chloride. *Metall. Trans. B Process Metall.* **1987**, *18*, 31–39. [[CrossRef](#)]

92. Parkman, R.H.; Charnock, J.M.; Bryan, N.D.; Livens, F.R.; Vaughan, D.J. Reactions of copper and cadmium ions in aqueous solution with goethite, lepidocrocite, mackinawite, and pyrite. *Am. Mineral.* **1999**, *84*, 407–419. [[CrossRef](#)]
93. Zhang, Y.; Li, W.; Cai, Y.; Qu, Y.; Pan, Y.; Zhang, W.; Zhao, K. Experimental investigation of the reactions between pyrite and aqueous Cu(I) chloride solution at 100–250 °C. *Geochim. Cosmochim. Acta* **2021**, *298*, 1–20. [[CrossRef](#)]
94. Ruiz, M.C.; Honores, S.; Padilla, R. Leaching kinetics of digenite concentrate in oxygenated chloride media at ambient pressure. *Metall. Trans. B Process Metall.* **1998**, *29*, 961–969. [[CrossRef](#)]
95. Peters, E. Oxygen utilization in hydrometallurgy: Fundamentals and basic principles. In Proceedings of the International Symposium, Impact of Oxygen on the Productivity of Non-Ferrous Metallurgical Processes, CIM, Winnipeg, MB, Canada, 23–26 August 1987; Kachaniwsky, G., Newman, C., Eds.; Pergamon Press: New York, NY, USA, 1987; pp. 151–164.
96. Heidel, C.; Tichomirowa, M. The role of dissolved molecular oxygen in abiotic pyrite oxidation under acid pH conditions—experiments with ¹⁸O-enriched molecular oxygen. *Appl. Geochem.* **2010**, *25*, 1664–1675. [[CrossRef](#)]
97. Tichomirowa, M.; Junghans, M. Oxygen isotope evidence for sorption of molecular oxygen to pyrite surface sites and incorporation into sulfate in oxidation experiments. *Appl. Geochem.* **2009**, *24*, 2072–2092. [[CrossRef](#)]
98. Sit, P.H.L.; Cohen, M.H.; Selloni, A. Interaction of oxygen and water with the (100) surface of pyrite: Mechanism of sulfur oxidation. *J. Phys. Chem. Lett.* **2012**, *3*, 2409–2414. [[CrossRef](#)]
99. Al-Harashsheh, M.; Kingman, S.; Al-Harashsheh, A. Ferric chloride leaching of chalcopyrite: Synergistic effect of CuCl₂. *Hydrometallurgy* **2008**, *91*, 89–97. [[CrossRef](#)]
100. Ferron, C.J.; Fleming, C.; O’Kane, P.T.; Dreisinger, D.B. Pilot plant demonstration of the Platsol process for the treatment of the NorthMet copper-nickel-PGM deposit. *Min. Eng.* **2002**, *54*, 33–39.
101. Dreisinger, D. Case study flowsheets: Copper–gold concentrate treatment. In *Developments in Mineral Processing: Advances in Gold Processing*, 1st ed.; Adams, M.D., Wills, B.A., Eds.; Elsevier B.V.: Amsterdam, The Netherlands, 2005; pp. 825–848.
102. Harris, G.B.; White, C.W.; Demopoulos, G.P.; Ballantyne, B. Recovery of copper from a massive polymetallic sulphide by high concentration chloride leaching. *Can. Metall. Q.* **2008**, *47*, 347–356. [[CrossRef](#)]
103. King, J.A.; Dreisinger, D.B.; Knight, D.A. The total pressure oxidation of copper concentrates. In *The Paul E. Queneau International Symposium Extractive Metallurgy of Copper, Nickel and Cobalt, Volume I: Fundamental Aspects*; Reddy, R.G., Weizenbach, R.N., Eds.; TMS: Warrendale, PA, USA, 1993; pp. 735–756.
104. Dreisinger, D.; Murray, W.; Hunter, D.; Baxter, K.; Ferron, J.; Fleming, C. The application of the Platsol™ Process to copper-nickel-cobalt-PGE/PGM concentrates from Polymet Mining’s NorthMet Deposit. In Proceedings of the ALTA 2005 Nickel/Cobalt 10 Conference, Perth, Australia, 16–18 May 2005; ALTA Metallurgical Services: Melbourne, Australia, 2005. 16p.
105. Defreyne, J.; Brace, T.; Miller, C.; Omena, A.; Matos, M.; Cobral, T. Commissioning UHC: A Vale Copper Refinery based on CESL technology. In *Hydrometallurgy 2008, Proceedings of the Sixth International Symposium*; Young, C.A., Taylor, P.R., Anderson, C.G., Eds.; SME: Littleton, CO, USA, 2008; pp. 357–366.
106. Antonijević, M.; Bogdanović, G.D. Investigation of the leaching of chalcopyritic ore in acidic solutions. *Hydrometallurgy* **2004**, *73*, 245–256. [[CrossRef](#)]
107. Abraitis, P.K.; Patrick, R.A.D.; Kelsall, G.H.; Vaughan, D.J. Acid leaching and dissolution of major sulphide ore minerals: Processes and galvanic effects in complex systems. *Mineral. Mag.* **2004**, *68*, 343–351. [[CrossRef](#)]
108. Fu, K.B.; Lin, H.; Mo, X.L.; Wang, H.; Wen, H.W.; Wen, Z.L. Comparative study on the passivation layers of copper sulphide minerals during bioleaching. *Int. J. Miner. Metall. Mater.* **2012**, *19*, 886–892. [[CrossRef](#)]
109. Nicol, M.; Basson, P. The anodic behaviour of covellite in chloride solutions. *Hydrometallurgy* **2017**, *172*, 60–68. [[CrossRef](#)]
110. Recalde Chiluiza, E.L.; Navarro Donoso, P. Chalcopyrite leaching in acidic chloride solution without sulphates. *J. Mex. Chem. Soc.* **2016**, *60*, 238–246. [[CrossRef](#)]
111. Papangelakis, V.G.; Demopoulos, G.P. Acid pressure oxidation of pyrite: Reaction kinetics. *Hydrometallurgy* **1991**, *26*, 309–325. [[CrossRef](#)]
112. Yu, P.H.; Hansen, C.K.; Wadsworth, M.E. A kinetic study of the leaching of chalcopyrite at elevated temperatures. *Metall. Trans.* **1973**, *4*, 2137–2144. [[CrossRef](#)]
113. Narita, E.; Lawson, F.; Han, K.N. Solubility of oxygen in aqueous electrolyte solutions. *Hydrometallurgy* **1983**, *10*, 21–37. [[CrossRef](#)]
114. Tromans, D. Oxygen solubility modeling in inorganic solutions: Concentration, temperature and pressure effects. *Hydrometallurgy* **1998**, *50*, 279–296. [[CrossRef](#)]
115. Tromans, D. Modeling oxygen solubility in water and electrolyte solutions. *Ind. Eng. Chem. Res.* **2000**, *39*, 805–812. [[CrossRef](#)]
116. Corriou, J.-P.; Kikindai, T. The aqueous oxidation of elemental sulfur and different chemical properties of the allotropic forms S_λ and S_μ. *J. Inorg. Nucl. Chem.* **1981**, *43*, 9–15. [[CrossRef](#)]
117. Collins, M.J.; Berezowsky, R.M.G.S.; Vardill, W.D.; Ketcham, V.J.; Stojsic, A. The Lihir Gold project: Pressure oxidation process development. In *Hydrometallurgy Fundamentals, Technology and Innovations*; Hiskey, J.B., Warren, G.W., Eds.; TMS: Littleton, CO, USA, 1993; Chapter 38; pp. 611–628.
118. Bartlett, P.D.; Davis, R.E. Reactions of elemental sulfur. II. The reaction of alkali cyanide with sulfur, and some single-sulfur transfer reactions. *J. Am. Chem. Soc.* **1958**, *80*, 2513–2516. [[CrossRef](#)]
119. Habashi, F.; Bauer, E.L. Aqueous oxidation of elemental sulfur. *Ind. Eng. Chem. Fundam.* **1966**, *5*, 469–471. [[CrossRef](#)]
120. Ghali, E.; Danapani, B.; Lewenstam, A. Electrodissolution of synthetic covellite in hydrochloric acid. *J. Appl. Electrochem.* **1982**, *12*, 369–376. [[CrossRef](#)]

121. Robinson, B.W. Sulphur isotope equilibrium during sulphur hydrolysis at high temperatures. *Earth Planet. Sci. Lett.* **1973**, *18*, 443–450. [[CrossRef](#)]
122. Smith, J.W. Isotopic fractionations accompanying sulfur hydrolysis. *Geochem. J.* **2000**, *34*, 95–99. [[CrossRef](#)]
123. Rimstidt, J.D.; Vaughan, D.J. Pyrite oxidation: A state-of-the-art assessment of the reaction mechanism. *Geochim. Cosmochim. Acta* **2003**, *67*, 873–880. [[CrossRef](#)]
124. Reedy, B.J.; Beattie, J.K.; Lawson, R.T. A vibrational spectroscopic ^{18}O tracer study of pyrite oxidation. *Geochim. Cosmochim. Acta* **1991**, *55*, 1609–1614. [[CrossRef](#)]
125. Usher, C.R.; Cleveland, C.A., Jr.; Strongin, D.R.; Schoonen, M.A. Origin of oxygen in sulfate during pyrite oxidation with water and dissolved oxygen: An in situ horizontal attenuated total reflectance spectroscopy isotope study. *Environ. Sci. Technol.* **2004**, *38*, 5404–5406. [[CrossRef](#)]
126. Gil-Lozano, C.; Davila, A.F.; Losa-Adams, E.; Fairén, A.G.; Gago-Duport, L. Quantifying Fenton reaction pathways driven by self-generated H_2O_2 on pyrite surfaces. *Sci. Rep.* **2017**, *7*, 43703. [[CrossRef](#)]
127. Li, Y.; Chen, J.; Chen, Y.; Zhao, C.; Zhang, Y.; Ke, B. Interactions of oxygen and water molecules with pyrite surface: A new insight. *Langmuir* **2018**, *34*, 1941–1952. [[CrossRef](#)]
128. Li, Y.; Chandra, A.P.; Gerson, A.R. Scanning photoelectron microscopy studies of freshly fractured chalcopyrite exposed to O_2 and H_2O . *Geochim. Cosmochim. Acta* **2014**, *133*, 372–386. [[CrossRef](#)]
129. Wei, Z.; Li, Y.; Gao, H.; Zhu, Y.; Qian, G.; Yao, J. New insights into the surface relaxation and oxidation of chalcopyrite exposed to O_2 and H_2O : A first-principles DFT study. *Appl. Surf. Sci.* **2019**, *492*, 89–98. [[CrossRef](#)]
130. Nicol, M.; Miki, H.; Velásquez-Yévenes, L. The dissolution of chalcopyrite in chloride solutions: Part 3. Mechanisms. *Hydrometallurgy* **2010**, *103*, 86–95. [[CrossRef](#)]
131. Corriou, J.-P.; Gely, R.; Viers, P. Thermodynamic and kinetic study of the pressure leaching of zinc sulfide in aqueous sulfuric acid. *Hydrometallurgy* **1988**, *21*, 85–102. [[CrossRef](#)]
132. Zhang, Q.; Dalla Lana, I.G.; Chuang, K.T.; Wang, H. Reactions between hydrogen sulfide and sulfuric acid: A novel process for sulfur removal and recovery. *Ind. Eng. Chem. Res.* **2000**, *39*, 2505–2509. [[CrossRef](#)]
133. Reid, M.; Papangelakis, V.G. New data on hematite solubility in sulphuric acid solution from 130 to 270 °C. In *Iron Control Technologies*; Durizac, J.E., Riveros, P.A., Eds.; MetSoc: Montreal, QC, Canada, 2006; pp. 673–686.
134. Liu, H.; Papangelakis, V.G.; Alam, M.S.; Singh, G. Solubility of hematite in H_2SO_4 solutions at 230–270 °C. *Can. Metall. Q.* **2003**, *42*, 199–208. [[CrossRef](#)]
135. Meyer, B. *Sulfur, Energy and Environment. Chapter 3 Properties*; Elsevier Scientific Publishing Company: Amsterdam, The Netherlands, 1977; pp. 38–79.
136. Tozawa, K.; Sasaki, K. Effect of co-existing sulphates on precipitation of ferric oxide from ferric sulphate solutions at elevated temperatures. In *Iron Control in Hydrometallurgy*; Dutrizac, J.E., Monhemius, A.J., Eds.; Ellis Horwood: Chichester, UK, 1986; pp. 454–476.
137. Munoz, P.B.; Miller, J.B.; Wadsworth, M.E. Reaction mechanism for the acid ferric sulphate leaching of chalcopyrite. *Metall. Trans. B Process Metall.* **1979**, *10B*, 149–158. [[CrossRef](#)]
138. Li, Y.; Wei, Z.; Qian, G.; Li, J.; Gerson, A.R. Kinetics and mechanisms of chalcopyrite dissolution at controlled redox potential of 750 mV in sulfuric acid solution. *Minerals* **2016**, *6*, 83. [[CrossRef](#)]
139. Yue, G.; Asselin, E. Kinetics of ferric ion reduction on chalcopyrite and its influence on leaching up to 150 C. *Electrochim. Acta* **2014**, *146*, 307–321. [[CrossRef](#)]
140. Hidalgo, T.; Kuhar, L.; Beinlich, A.; Putnis, A. Kinetic study of chalcopyrite dissolution with iron (III) chloride in methanesulfonic acid. *Miner. Eng.* **2018**, *125*, 66–74. [[CrossRef](#)]
141. Baba, A.A.; Ayinla, K.I.; Adekola, F.A.; Bale, R.B.; Ghosh, M.K.; Alabi, A.G.; Sheik, A.R.; Folorunso, I.O. Hydrometallurgical application for treating a Nigerian chalcopyrite ore in chloride medium: Part I. Dissolution kinetics assessment. *Int. J. Miner. Metall. Mater.* **2013**, *20*, 1021–1028. [[CrossRef](#)]
142. Baba, A.A.; Ayinla, K.I.; Bale, R.B.; Adekola, F.A. Quantitative leaching of a Nigerian chalcopyrite ore by nitric acid. *Bayero J. Pure Appl. Sci.* **2014**, *7*, 115–121.
143. Sokić, M.D.; Marković, B.; Živković, D. Kinetics of chalcopyrite leaching by sodium nitrate in sulphuric acid. *Hydrometallurgy* **2009**, *95*, 273–279. [[CrossRef](#)]
144. Bobeck, G.; Su, H. The kinetics of dissolution of sphalerite in ferric chloride solution. *Metall. Trans. B* **1985**, *16*, 413–424. [[CrossRef](#)]
145. Qian, G.; Li, J.; Li, Y.; Gerson, A.R. Probing the effect of aqueous impurities on the leaching of chalcopyrite under controlled conditions. *Hydrometallurgy* **2014**, *149*, 195–209. [[CrossRef](#)]
146. Fuentes, G.; Viñals, J. Hydrothermal purification and enrichment of Chilean copper concentrates. The behavior of bornite, covellite, pyrite and chalcopyrite. In *Proceedings of the Pressure Hydrometallurgy 2012, 42nd Annual Hydrometallurgy Meeting, Niagara Falls, ON, Canada, 30 September–3 October 2012*; Collins, M.J., Filippou, D., Harlamovs, J., Peek, E., Eds.; MetSoc on behalf of the Canadian Institute of Mining, Metallurgy and Petroleum: Montreal, QC, Canada, 2012; pp. 257–267.
147. Petrović, S.J.; Bogdanović, G.D.; Antonijević, M.M. Leaching of chalcopyrite with hydrogen peroxide in hydrochloric acid solution. *Trans. Nonferrous. Met. Soc. China* **2018**, *28*, 1444–1455. [[CrossRef](#)]

148. He, G.; Zhao, Z.; Wang, X.; Li, J.; Chen, X.; He, L.; Liu, X. Leaching kinetics of scheelite in hydrochloric acid solution containing hydrogen peroxide as complexing agent. *Hydrometallurgy* **2014**, *144*, 140–147. [[CrossRef](#)]
149. Prosser, A.P. Review of uncertainty in the collection and interpretation of leaching data. *Hydrometallurgy* **1996**, *41*, 119–153. [[CrossRef](#)]

Disclaimer/Publisher’s Note: The statements, opinions and data contained in all publications are solely those of the individual author(s) and contributor(s) and not of MDPI and/or the editor(s). MDPI and/or the editor(s) disclaim responsibility for any injury to people or property resulting from any ideas, methods, instructions or products referred to in the content.